

MapTab: Can MLLMs Master Constrained Route Planning?

Ziqiao Shang^{1,2†} Lingyue Ge^{1,2†} Yang Chen^{1,2} Shi-Yu Tian^{1,2} Zhenyu Huang^{1,2} Wenbo Fu^{1,2}
Yu-Feng Li^{1,2} Lan-Zhe Guo^{1,2*}

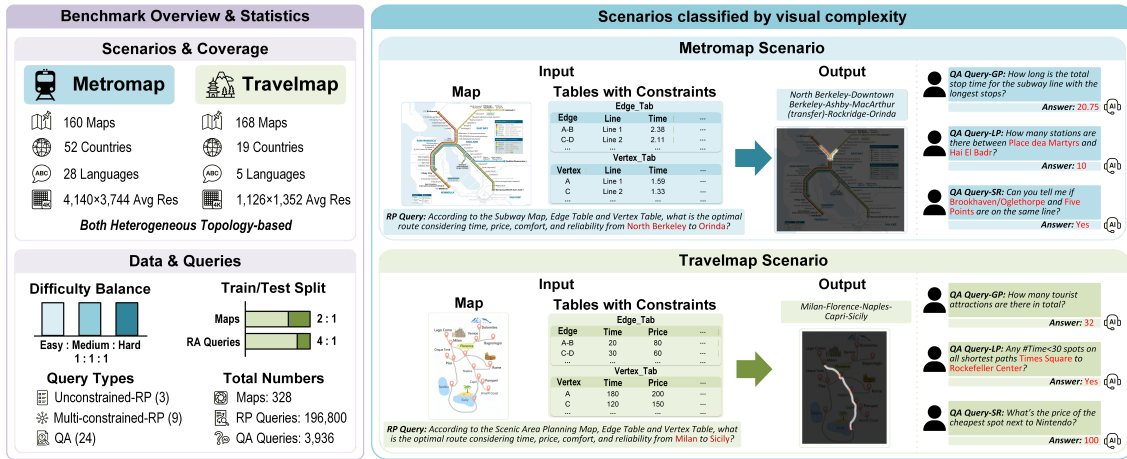


Figure 1. Composition and Statistical Overview of the MapTab Benchmark. MapTab features 328 high-resolution maps across Metromap and Travelmap scenarios, providing 196,800 RP queries and 3,936 QA queries.

Abstract

Systematic evaluation of Multimodal Large Language Models (MLLMs) is crucial for advancing Artificial General Intelligence (AGI). However, existing benchmarks remain insufficient for rigorously assessing their constrained reasoning capabilities. To bridge this gap, we introduce **MapTab**, a multimodal benchmark specifically designed to evaluate constrained reasoning in MLLMs via route planning tasks. MapTab requires MLLMs to perceive and ground visual cues from map images alongside route attributes (e.g., Time, Price) from structured tabular data. The benchmark encompasses two scenarios: **Metromap**, covering metro networks in **160** cities across **52** countries, and **Travelmap**, depicting **168** representative tourist attractions

from **19** countries. In total, MapTab comprises **328** images, **196,800** route planning queries, and **3,936** QA queries, all incorporating 4 key constraints: Time, Price, Comfort, and Reliability. Extensive evaluations across 15 representative MLLMs reveal that current models face substantial challenges in constrained multimodal reasoning. Notably, under conditions of limited visual perception, multimodal collaboration often underperforms compared to unimodal approaches. We believe MapTab provides a challenging and realistic testbed to advance the systematic evaluation of MLLMs. Our code is available at <https://github.com/Ziqiao-Shang/MapTab>.

1. Introduction

Multimodal large language models (MLLMs) (Bai et al., 2025a) integrate cross-modal representations and techniques such as visual chain-of-thought (Hu et al., 2024) and multi-dimensional perception (Yu et al., 2025), enabling remarkable reasoning capabilities and applications in complex decision-making (Hong et al., 2025), game agents (Tan et al., 2025b), and autonomous driving (Lu et al., 2025a). Accordingly, systematic evaluation of

[†] These authors contributed equally. ¹National Key Laboratory for Novel Software Technology, Nanjing University, Nanjing, China ²School of Intelligence Science and Technology, Nanjing University, Suzhou, China. Correspondence to: Lan-Zhe Guo <guolz@lamda.nju.edu.cn>.

MLLMs has become a critical yet challenging research direction (Lu et al., 2023; Qiao et al., 2025a; Li et al., 2025a). Early benchmarks, including MMMU (Yue et al., 2024) and V*-Bench (Wu & Xie, 2024) *et al.*, focused on basic and structured visual reasoning, while maps naturally integrating topology and semantics, have been increasingly adopted to evaluate MLLMs in multi-scale geographic and complex topological reasoning, as reflected in benchmarks such as Mapbench (Xing et al., 2025), ReasonMap (Feng et al., 2025d), and RewardMap (Feng et al., 2025c) *et al.*

Despite these advances, existing benchmarks remain insufficient to characterize constrained multimodal reasoning. Such reasoning requires models to simultaneously satisfy multiple constraints, temporal, spatial, and resource based, within a unified framework to support robust and personalized decision-making. Map-based multimodal route planning (RP) offers a representative evaluation setting, as maps provide explicit structured information that enables systematic assessment of long-tracing reasoning. RP is inherently multi-factor and strongly constrained, demanding the joint optimization of efficiency, cost, comfort, and reliability across diverse user preferences. These trade-offs, which vary systematically across user groups, closely mirror real-world industrial route planning systems and place substantial demands on models’ holistic reasoning and constraint-handling capabilities.

Motivated by these observations, we propose MapTab, a multimodal evaluation framework based on *vision-structured data* collaborative modeling for heterogeneous topological reasoning under complex constraints. As shown in Fig. 1, MapTab covers two scenarios, Metromap and Travelmap, comprising a total of **328** images, where Metromap includes metro maps from **52** countries and **160** cities worldwide, and Travelmap consists of travel maps from **19** countries depicting **168** representative tourist attractions. Since a single map image cannot incorporate essential quantitative attributes such as time, price, *et al.*, which are crucial for constraint-based decision-making, we introduce two complementary tables, Vertex_tab and Edge_tab, to store these attributes in a structured format. Moreover, representing the map as a graph structure allows for a clear depiction of both the attributes of stations/attractions and the relationships between them, aligning with the topological nature of the problem. For the core RP task, MapTab includes **16,400** origin-destination pairs, yielding **196,800** unconstrained and multi-constrained RP queries. Furthermore, MapTab offers 3,936 QA queries, which are designed to support a comprehensive analysis of the benchmark characteristics.

MapTab introduces substantial improvements over existing benchmarks and fills several critical gaps in current evaluation frameworks: 1) **Multi-constraint evaluation:**

To address the lack of benchmarks incorporating realistic constraints, MapTab integrates multiple constraints into RP tasks, enabling MLLMs to generate personalized and robust decisions. 2) **Topology-focused reasoning:** To overcome distractions from redundant visual details in traditional maps, MapTab uses metro and scenic-area topology maps with time, cost, comfort, and reliability encoded in a heterogeneous graph, reducing perceptual complexity and isolating reasoning performance. 3) **Vision-structured data collaboration:** To overcome the reliance on image and unstructured text modalities in existing datasets, MapTab combines map images with tabular node attributes to assess joint visual-structured reasoning, ranging from complementary reasoning between maps and node attributes when edge-based topology is not provided, to selective exploitation of topological information from multiple modalities when edge_tab are available.

In summary, our contributions are threefold:

- **Multimodal multi-constraint benchmark:** MapTab first combines visual and structured data in route planning tasks to assess MLLMs’ reasoning over heterogeneous, multi-constraint graphs.
- **Large-scale dual-scenario benchmark:** MapTab comprises a total of **328** maps, with Metromap images spanning **52** countries and **160** cities, and Travelmap images covering **19** countries and **168** tourist attractions. It also includes **16,400** origin-destination pairs, **196,800** RP queries, and **3,936** QA queries, offering a comprehensive benchmark for analysis.
- **Comprehensive MLLM evaluation:** We assess 15 long-context MLLMs on constraints, multimodal collaboration, and reasoning chains, revealing performance limits under multi-constraint settings.

2. Task Definition

Given an image I , an edge information table (Edge_tab E), a node information table (Vertex_tab V), and a route planning query Q , the objective of MLLMs is to generate an optimal planned route r^* based on these inputs.

Specifically, the **input** (I, E, V, Q) is defined as follows: I denotes the input metro map (or scenic route map); $E = (\hat{T}_e, \hat{P}_e, \hat{C}_e, \hat{R}_e)$ represents Edge_tab, which records the normalized time \hat{T}_e , price \hat{P}_e , comfort level \hat{C}_e , and reliability \hat{R}_e for each metro line (or inter-attraction commuting path) in the image; $V = (\hat{T}_v, \hat{P}_v, \hat{C}_v, \hat{R}_v)$ represents Vertex_tab, which stores the same multi-dimensional attributes for each metro station (or scenic spot); the text query Q is a multi-constraint query that includes starting point s , destination point t and user’s constraints, where s and t both corresponding to metro stations (or scenic spots) in the image. The **output** is an optimal planned route r^* , represented as

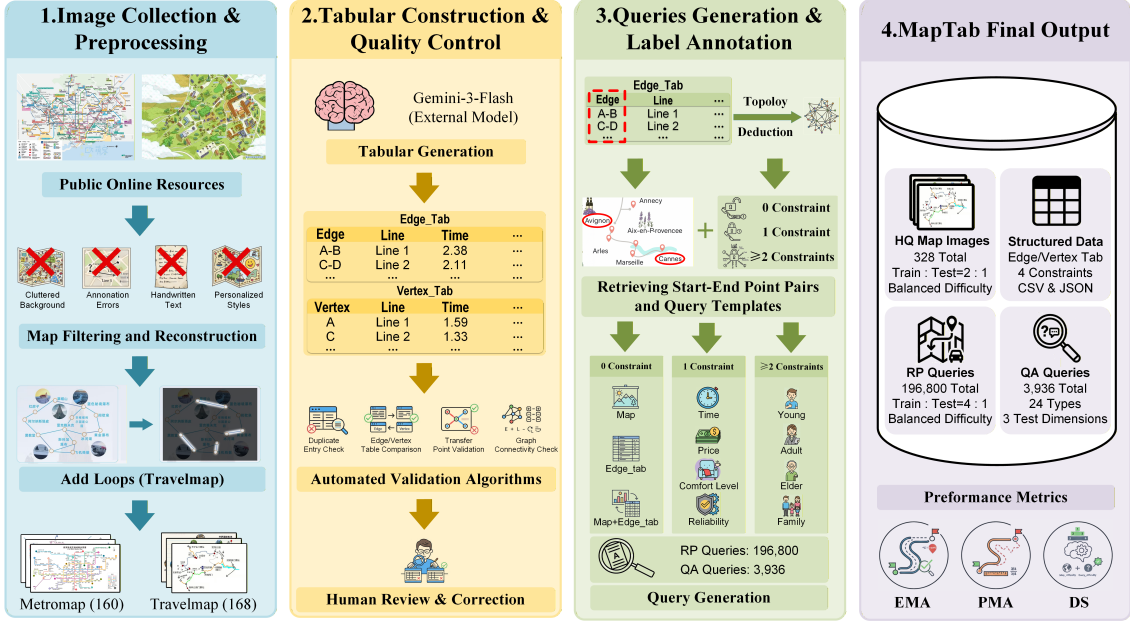


Figure 2. Schematic overview of the MapTab construction pipeline, comprising 5 main steps: Image Collection & Preprocessing, Tabular Construction, Quality Control, Query Generation, and Label Annotation.

an ordered sequence of nodes starting from s and ending at t , i.e., $r^* = (v_1, v_2, \dots, v_k)$, where $v_1 = s$ and $v_k = t$.

Optimization Objective: Given a starting station/spot s and a target station/spot t , the objective is to find the optimal route r^* that minimizes the overall path cost:

$$r^* = \arg \min_{r \in \mathcal{R}(s,t)} \left[w_1 T(r, \hat{T}_e, \hat{T}_v) + w_2 P(r, \hat{P}_e, \hat{P}_v) + w_3 (1 - C(r, \hat{C}_e, \hat{C}_v)) + w_4 (1 - R(r, \hat{R}_e, \hat{R}_v)) \right] \quad (1)$$

where $\mathcal{R}(s,t)$ denotes the set of all feasible routes from s to t . $T(r, \hat{T}_e, \hat{T}_v)$, $P(r, \hat{P}_e, \hat{P}_v)$, $1 - C(r, \hat{C}_e, \hat{C}_v)$, and $1 - R(r, \hat{R}_e, \hat{R}_v)$ denote the Time, Price, Comfort Level, and Reliability costs of route r , respectively. The weights w_1, w_2, w_3, w_4 balance the path cost factors to minimize the overall cost.

3. MapTab Building Pipeline

This study introduces MapTab, a multimodal benchmark designed to evaluate MLLMs on multi-constraint heterogeneous graph reasoning across two scenarios, Metromap and Travelmap (see Section 3.1). As shown in Fig. 2, we curate 328 high-quality maps (see Section 3.2.1) and use structured tables to store multi-dimensional node and edge attributes (see Section 3.2.2), with a dual-track quality control process ensuring the reliability of the benchmark and its annotations (see Section 3.2.3). Using deterministic algorithms, we generate a complete set of queries for RP tasks and QA tasks, evaluating MLLM reasoning robust-

ness with varied instruction templates (see Section 3.3).

3.1. Benchmark Statistics

MapTab comprises two scenarios, Metromap and Travelmap, both represented in the form of topological graphs. Metromap includes 160 maps covering 52 countries, involving 32 native languages, with images rendered in 28 languages and an average resolution of $4,140 \times 3,744$ pixels. Travelmap consists of 168 maps covering 19 countries, involving 15 native languages, with images rendered in 5 languages and an average resolution of $1,126 \times 1,352$ pixels, containing relatively less information than Metromap. Maps in both scenarios are categorized into three difficulty levels, easy, medium, and hard, with a strictly balanced ratio of 1:1:1 across difficulty levels. The image split between the training and test sets follows a 2:1 ratio (218 images for training and 110 images for testing).

MapTab defines a total of 16,400 base origin-destination pairs (8,000 for Metromap and 8,400 for Travelmap), which are split into training and test sets at a ratio of 4:1 (13,120 for training and 3,280 for testing). As a result, the average number of origin-destination pairs per training image is approximately twice that of the test images. Queries are generated based on these origin-destination pairs and include three types of unconstrained queries and nine types of multi-constrained queries, yielding a total of 196,800 evaluation queries. These queries are evenly distributed across the three difficulty levels (easy, medium, and hard) with a 1:1:1 ratio. In addition, MapTab contains 3,936 QA queries, with 12 questions per image. QA queries are not split into

training and test sets and are not assigned difficulty levels. Instead, all images are treated as test data and are used solely for MLLM evaluation and benchmark characteristic analysis.

3.2. Data Collection and Preprocessing

3.2.1. METROMAP/TRAVELMAP IMAGE COLLECTION AND PREPROCESSING

To ensure data quality, we collect map images with clear backgrounds and high resolution from multiple public online sources whenever possible. During preprocessing, we discard maps with cluttered backgrounds, incorrect annotations, handwritten content, or overly personalized designs, and regenerate or manually correct them as needed. For Travelmap, in cases where direct routes exist between distant attractions but are not explicitly connected, we randomly add loop connections to enhance the completeness of the topological structure. All images are publicly sourced and properly licensed.

3.2.2. CONSTRAINT CONDITION TABULAR CONSTRUCTION

Compared to the "image + unstructured text" paradigm, the "image + table" paradigm provides a strong structural prior. In RP tasks, tables encode node and edge attributes in a low-entropy, high signal-to-noise manner, effectively avoiding the semantic ambiguity and redundancy inherent in natural language descriptions. Specifically, by combining Gemini-3-Flash, validation algorithms, and manual correction (see Section 3.2.3), we generate **Edge_tab** and **Vertex_tab**, enabling multi-constraint information to be modeled in the form of heterogeneous graphs.

Metromap is designed to simulate real-world urban commuting scenarios. Its **Edge_tab** includes six key attributes: Edge, Line, Time, Price, Comfort Level, and Reliability. The Edge column follows the topological annotation format of FarPlanning (Cao et al., 2023), while the numerical design of the remaining attributes is informed by metro operational characteristics and user experience (see Appendix E.1.1). On this basis, **Vertex_tab** introduces an additional Transfer Time dimension to supplement the time cost not covered by the Time column during transfers (see Appendix E.1.2). In contrast, Travelmap focuses on semantic evaluation and user psychological modeling. Compared with Metromap, it removes the Line and Transfer Time dimensions, retaining only five columns, Edge, Time, Price, Comfort Level, and Reliability, in both **Edge_tab** and **Vertex_tab**. The numerical values in Travelmap are primarily designed with reference to rating systems in real-world travel applications and map-provided indicative information (see Appendix E.1.3 and E.1.4). MapTab provides data in both CSV and JSON formats to explore the impact of tab-

ular formats on experimental outcomes (see Appendix F.5).

3.2.3. QUALITY CONTROL

To ensure the accuracy of **Edge_tab** and **Vertex_tab**, we implement dedicated validation algorithms for Metromap and Travelmap (see Appendix B.3 and B.4) to pre-verify outputs from Gemini-3-Flash. Each result is then manually checked, ensuring reliability across the entire data pipeline.

3.3. Queries Construction

Our queries consist of RP queries and QA queries, which together constitute essential inputs to the model. RP queries are designed to assess its ability to handle constraint-based reasoning and optimization tasks. On the other hand, QA queries evaluate model performance in answering diverse questions based on maps. RP queries comprise 12 distinct categories, including 3 unconstrained and 9 constraint-aware variants (see Appendix D.1), whereas QA queries span a total of 24 categories (see Appendix D.2). The construction of RP queries and QA queries is based on the previously generated **Edge_tab** and **Vertex_tab**, and is fully automated using deterministic Python programs. Under the assumption that **Edge_tab** and **Vertex_tab** themselves contain no structural or semantic errors, the generated queries exhibit verifiable completeness in terms of logical consistency and formal correctness, and are theoretically free from additional construction-induced bias or noise. This section focuses on the RP query construction process, and details of QA query construction are provided in Appendix B.2.

3.3.1. QUESTION GENERATION

We divide RP tasks into **unconstrained** and **constrained** categories, using a unified route generation logic for both Metromap and Travelmap. For unconstrained tasks, we evaluate models' parsing capabilities using three input modalities: *Map only*, *Edge_tab only*, and *Map + Edge_tab*, where **Edge_tab** contains only *Edge Column* without constraints. To reduce semantic bias, each modality is paired with five distinct instruction templates (Direct Optimization, Graph-theoretic, Instruction-seeking, User-oriented, and Constraint-explicit; see Appendix D.1), applied cyclically across questions and origin-destination pairs. Origin-destination pairs are sampled from the topological graph of **Edge_tab** (Appendix B.2) and shortest paths are computed with *Dijkstra* algorithm until quotas are met. Each route contains at least three stations to guarantee meaningful tasks.

For constrained tasks, we define nine scenarios, including four single-constraint settings (Time, Price, Comfort Level, Reliability) and five multi-constraint combinations. For multi-constraint tasks with **Map + Edge_tab + Vertex_tab**,

MapTab simulates diverse user preferences: younger users prioritize time efficiency and cost (Time + Price + Reliability), middle-aged users balance efficiency and comfort (Time + Comfort Level + Reliability), older users emphasize affordability and travel comfort (Price + Comfort Level + Reliability), and families consider all four factors. With Map + Vertex2_tab, where Vertex2_tab integrates partial Edge_tab information to reduce reliance on topological cues (see Appendix E.2), only the full combination of all four factors is used. During evaluation, only relevant columns are given to the model to reduce context length.

3.3.2. REFERENCE ROUTE COLLECTION AND LABEL ANNOTATION

The generation of reference routes follows a similar strategy to origin-destination sampling. First, the graph topology is derived from Edge_tab, and all shortest paths are computed using *Dijkstra* algorithm. For constrained scenarios, the key difference from unconstrained scenarios lies in the preprocessing of per-dimension weights, which are normalized to a unified scale and combined via weighted aggregation to compute route scores (see Appendix E.2). For transfer stations, a “(transfer)” marker is appended to the station name, resulting in route representations such as “A-B(transfer)-C”. Finally, four aggregate metrics, Total_Time, Total_Price, Average_Comfort Level, and Average_Reliability, are appended to each route label to support ablation studies on constraints.

4. Experiments

4.1. Experimental Setups

This section presents a systematic evaluation of 15 state-of-the-art long-context VLM on MapTab, comparing the performance of open-source and closed-source models on RP tasks across two scenarios. Experimental details for QA tasks are provided in Appendix F.2.

Evaluated Models. We systematically evaluate multiple categories of multimodal large language models (MLLMs), which are divided according to their reasoning mechanisms into general instruction-following models and reasoning-enhanced models with long chain-of-thought (Long-CoT) capabilities. The former category includes the Qwen3-VL-Instruct series (2B, 8B, 30B-A3B, 32B) (Bai et al., 2025a), Qwen2.5-VL-Instruct (7B) (Bai et al., 2025b), Phi-3.5-Vision-Instruct (4B) (Abdin et al., 2024a), Phi-4-Multimodal-Instruct (6B) (Abdin et al., 2024b), InternVL3-Instruct (8B) (Zhu et al., 2025), GPT-4o (Hurst et al., 2024), GPT-4.1 (OpenAI, 2025a), and Gemini-3-Flash-Preview (Google, 2025). The latter category includes Qwen3-VL-Thinking (8B, 32B) (Bai et al., 2025a), Doubao-Seed-1-6-251015-Thinking (ByteDance

Seed Team, 2025), and Qwen3-VL-Plus-Thinking (Bai et al., 2025a). To ensure fairness and reproducibility, we adopt unified protocols for model selection, deployment, parameter configuration, and multimodal input preprocessing. Detailed settings are provided in Appendix F.1.

Metrics. For model performance evaluation, RP tasks are assessed using three metrics:

- **Exact Match Accuracy (EMA):** EMA evaluates whether the generated route exactly matches the reference path in station order and content, allowing minor spelling variations.
- **Partial Match Accuracy (PMA):** PMA measures the proportion of the longest contiguous correct prefix from the origin, reflecting partial path consistency.
- **Difficulty-aware Score (DS):** DS incorporates task difficulty by weighting exact matches according to the combined Map_Difficulty and Query_Difficulty levels, thereby characterizing model robustness on harder instances.

Detailed definitions of these metrics are provided in Appendix C.1. In addition, we design multiple indicators to characterize Map_Difficulty and Query_Difficulty. Further details are given in Appendix C.2.

4.2. Experimental Results

4.2.1. PERFORMANCE OF MLLMS ON RP

Table 1 systematically reveals the reasoning capabilities and performance limitations of MLLMs on constrained heterogeneous graph tasks from four perspectives: modality comparison, constraint effects, multimodal collaboration, and explicit reasoning chains.

Observation 1: Visual perception bottlenecks lead to over-reliance on structured data. Across models, Map-only inputs consistently yield lower performance than Edge_tab-only inputs, reflecting the difficulty of recovering accurate topology from pixel-level map images, especially in the presence of crossings or overlapping structures. Moreover, in dense or low-resolution settings, even basic optical character recognition (OCR) and entity identification become unreliable.

Observation 2: Constraints exert a dual effect on model reasoning. Introducing constraints generally increases reasoning burden and degrades performance. However, we observe a counterintuitive anchoring effect: in visually dense MetroMap scenarios, Map + Vertex2_tab substantially outperforms the Map-only setting. This improvement likely arises because Vertex2_tab provides reliable symbolic anchors that correct OCR and entity recognition errors, with

MapTab: Can MLLMs Master Constrained Route Planning?

Table 1. Evaluation results of various Multimodal Large Language Models (MLLMs) on the TravelTab path planning task **MetroMap** and **TravelMap** scenarios. EMA, PMA, and DS denote Exact Match Accuracy, Partial Match Accuracy, and Difficulty-aware Score, respectively. Map-only: map information only; Edge_tab-only: edge data only; Map+Edge_tab: map and edge data; Map+Edge_tab+Vertex_tab: map, edge, and vertex data; Map+Vertex2_tab: map and merged vertex data (Vertex2_tab). Bold values represent the best performance within open-source and closed-source groups, respectively.

Model	Type	Map-only			Edge-only			Map+Edge			Map+Edge+Vertex			Map+Vertex2		
		EMA	PMA	DS	EMA	PMA	DS	EMA	PMA	DS	EMA	PMA	DS	EMA	PMA	DS
<i>Scenario: MetroMap</i>																
<i>Open-source Models</i>																
Qwen3-VL-8B-Instruct	Instruct	2.75	17.58	67	25.69	46.44	1018	21.25	41.30	785	19.31	39.31	728	4.69	21.87	137
Qwen3-VL-8B-Thinking	Thinking	5.12	20.99	132	31.69	49.76	1276	38.00	57.06	1669	23.75	41.69	948	6.38	22.93	194
Qwen3-VL-2B-Instruct	Instruct	0.94	15.14	26	9.88	27.61	371	6.63	23.85	232	7.00	26.91	289	2.00	17.82	58
Qwen2.5-VL-7B-Instruct	Instruct	0.94	15.02	21	14.00	31.20	535	11.69	28.32	441	7.94	20.77	318	3.38	18.09	101
Phi-3.5-Vision-Instruct-4B	Instruct	0.06	10.40	1	10.87	27.92	402	6.63	22.14	208	2.75	12.27	99	0.81	12.94	13
Phi-4-Multimodal-Instruct-6B	Instruct	0.00	9.75	0	2.13	12.52	66	2.13	11.78	85	1.75	9.51	52	0.44	9.02	7
InternVL3-8B-Instruct	Instruct	0.13	13.98	2	10.50	29.57	414	12.81	31.83	488	9.00	24.73	377	1.75	17.0	68
Qwen3-VL-30B-A3B-Instruct	Instruct	3.31	19.26	102	23.69	44.33	961	22.56	43.58	914	19.00	40.03	724	6.75	26.22	218
Qwen3-VL-32B-Instruct	Instruct	6.31	22.23	181	31.87	54.45	1270	32.12	54.54	1339	28.50	50.06	1181	6.56	24.43	187
Qwen3-VL-32B-Thinking	Thinking	13.31	29.43	437	31.81	54.94	1276	44.12	62.77	2078	26.56	51.48	1060	9.19	28.89	278
<i>Closed-source Models</i>																
GPT-4o	Instruct	6.63	25.61	205	42.38	64.07	2112	40.69	62.40	1944	35.63	55.51	1630	11.31	31.11	398
GPT-4.1	Instruct	7.94	25.52	235	48.56	67.07	2523	46.81	65.18	2413	41.81	62.88	2038	14.06	35.98	515
Gemini-3-Flash-Preview	Instruct	37.06	57.15	2046	74.75	84.99	5345	73.06	83.37	5171	69.19	76.14	4765	53.87	65.84	3294
Doubao-Seed-1-6-251015-w/o	No-Thinking	8.13	24.60	233	46.94	66.98	2394	48.06	66.95	2533	40.56	62.11	2088	13.81	35.61	494
Doubao-Seed-1-6-251015-Thinking	Thinking	12.06	30.49	461	74.38	86.23	4996	74.00	85.68	4964	76.06	83.41	5029	22.03	42.48	984
Qwen-VL-Plus-w/o	No-Thinking	4.81	21.83	133	36.88	58.69	1643	38.25	58.59	1706	31.62	52.92	1355	6.94	27.69	229
Qwen-VL-Plus-Thinking	Thinking	10.75	29.11	349	61.50	76.62	3576	62.19	76.42	3648	45.75	64.46	2318	16.38	37.44	582
<i>Scenario: TravelMap</i>																
<i>Open-source Models</i>																
Qwen3-VL-8B-Instruct	Instruct	19.29	42.50	1190	44.05	61.66	3051	43.33	61.39	3008	34.52	55.56	2330	15.65	40.97	869
Qwen3-VL-8B-Thinking	Thinking	22.62	45.94	1345	74.17	82.41	5319	82.68	88.54	6268	33.15	55.60	2088	12.74	38.10	705
Qwen3-VL-2B-Instruct	Instruct	8.45	34.30	500	11.25	32.35	763	19.17	45.68	1210	12.14	40.47	787	3.15	30.69	164
Qwen2.5-VL-7B-Instruct	Instruct	7.68	30.48	431	21.07	38.15	1322	24.82	42.02	1508	15.60	37.47	902	4.70	28.84	235
Phi-3.5-Vision-Instruct-4B	Instruct	0.12	20.00	8	12.20	34.81	778	9.82	31.87	620	4.46	23.21	263	1.31	22.68	81
Phi-4-Multimodal-Instruct-6B	Instruct	0.42	19.26	21	7.20	17.63	479	5.30	15.93	318	1.73	9.36	115	1.43	18.96	63
InternVL3-8B-Instruct	Instruct	6.61	29.21	309	29.58	49.69	1821	29.40	50.16	1865	13.57	36.78	933	2.50	24.28	136
Qwen3-VL-30B-A3B-Instruct	Instruct	17.86	44.15	1098	50.95	65.36	3458	53.75	67.71	3747	38.45	58.02	2738	9.70	37.93	578
Qwen3-VL-32B-Instruct	Instruct	36.90	57.44	2431	64.52	76.16	4704	68.39	78.99	5184	52.56	69.18	3770	21.67	47.34	1299
Qwen3-VL-32B-Thinking	Thinking	39.17	58.84	2650	69.76	79.60	5149	91.79	94.55	7287	42.32	62.99	2931	19.94	46.73	1201
<i>Closed-source Models</i>																
GPT-4o	Instruct	16.85	40.98	930	65.06	75.84	4651	62.74	74.11	4467	46.07	63.07	3069	12.08	38.07	675
GPT-4.1	Instruct	20.30	43.24	1226	74.82	82.98	5571	70.89	79.84	5211	54.70	69.59	3917	15.06	40.67	862
Gemini-3-Flash-Preview	Instruct	60.00	73.20	4469	98.27	98.38	8190	94.40	94.87	7757	78.51	82.40	6459	43.51	60.11	3250
Doubao-Seed-1-6-251015-w/o	No-Thinking	33.04	54.15	2193	73.51	82.16	5425	76.85	84.04	5812	56.25	71.46	4031	25.48	49.54	1610
Doubao-Seed-1-6-251015-Thinking	Thinking	38.45	58.46	2735	98.39	98.87	8178	97.86	98.47	8127	83.15	89.08	6672	25.30	48.90	1678
Qwen-VL-Plus-w/o	No-Thinking	30.60	52.64	1935	64.23	76.45	4656	69.64	79.78	5133	53.99	70.07	3842	22.92	47.65	1417
Qwen-VL-Plus-Thinking	Thinking	38.27	58.94	2539	64.35	76.53	4670	94.23	96.04	7570	56.19	70.84	4042	23.21	47.18	1481

the benefits of accurate entity grounding outweighing the added reasoning cost.

Observation 3: Multiple effects of multimodal interaction. To investigate the synergy between visual and structured data, we compare Edge_tab-only versus Map + Edge_tab across Metromap and Travelmap scenarios. For Instruct models, in the visually dense Metromap tasks, Map + Edge_tab underperforms Edge_tab alone due to interference from complex visuals that disrupt text-based CoT reasoning. However, in simpler Travelmap scenarios, multimodal inputs generally enhance performance, highlighting the limited robustness of cross-modal integration under high visual complexity. For Thinking models, all Qwen-series Thinking models show notable improvements, reflecting effective synergy between text and visual inputs through CoT, whereas the Doubao model performs similarly across modalities, indicating that it reaches information saturation with text alone, and CoT does not further extend its reasoning capability.

Observation 4: Explicit reasoning chains exhibit a

double-edged effect. Explicit reasoning chains generally enhance performance for complex, compositional tasks. However, in simpler constrained Travelmap scenarios, Qwen3-VL-32B-Thinking slightly underperforms its Instruct variant. This observation further supports the hypothesis that chain-of-thought prompting cannot surpass a model’s intrinsic upper bound of reasoning capability.

4.2.2. ABLATION STUDY FOR CONSTRAINTS

As shown in Tables 2 and 3, we conduct ablation studies on RP tasks to evaluate the impact of constraints on path selection. In Table 2, using Qwen3-VL-8B-Instruct and fixing both the start and end stations, the changes between constrained paths and shortest paths can be categorized into three types after introducing constraints: 1) **Fully Repeat (FR)**: The shortest path is unique, and the constrained path remains unchanged. 2) **Partially Repeat (PR)**: Multiple shortest paths exist, and the constrained path matches one of them. 3) **Not Repeat (NR)**: The shortest path is unique, but the constrained path differs. When multiple shortest paths exist, no misaligned paths are observed.

MapTab: Can MLLMs Master Constrained Route Planning?

Table 2. Ablation studies of RP under different constraint conditions in the Metromap and Travelmap scenarios. Query types are categorized into Fully Repeat (FR), Partially Repeat (PR), and Not Repeat (NR), aiming to examine the degree of deviation between the constrained paths and the shortest paths after constraint introduction. *Num* denotes the number of queries in each category.

Metromap												
Constraint Settings	FR			PR			NR			All		
	Num	EMA	PMA	Num	EMA	PMA	Num	EMA	PMA	Num	EMA	PMA
Time-Only	1162	26.59	46.75	104	1.92	16.36	334	1.80	21.34	1600	19.81	39.47
Price-Only	1100	30.91	51.05	107	0	13.87	393	3.31	25.94	1600	22.06	42.40
Comfort_Level-Only	1114	25.31	46.24	95	0	16.20	391	2.56	23.81	1600	18.25	38.97
Reliability-Only	1162	25.73	45.57	132	0	13.84	306	3.59	27.69	1600	19.38	39.53
Time+Price+Reliability	1213	24.73	44.79	132	1.52	15.44	255	2.35	23.12	1600	19.25	38.91
Time+Comfort_Level+Reliability	1224	24.51	44.74	131	1.53	15.22	245	1.63	23.31	1600	19.13	39.04
Price+Comfort_Level+Reliability	1151	26.06	47.06	122	0	12.68	327	3.36	26.23	1600	19.44	40.18
Time+Price+Comfort_Level+Reliability	1236	24.35	44.42	134	0.75	17.14	230	3.04	24.82	1600	19.31	39.31
Total_num	9362	25.96	46.26	957	0.73	15.08	2481	2.74	24.59	12800	19.58	39.73

Travelmap												
Constraint Settings	FR			PR			NR			All		
	Num	EMA	PMA	Num	EMA	PMA	Num	EMA	PMA	Num	EMA	PMA
Time-Only	1297	36.24	50.57	262	8.40	29.30	121	9.09	29.02	1680	29.94	45.70
Price-Only	1332	45.20	62.32	277	13.36	36.56	71	15.49	39.44	1680	38.69	57.11
Comfort_Level-Only	1311	39.05	59.99	271	18.45	44.78	98	12.24	38.47	1680	34.17	56.28
Reliability-Only	1309	43.32	62.76	245	19.18	44.42	126	8.73	36.12	1680	37.20	58.08
Time+Price+Reliability	1354	39.81	59.41	275	12.36	37.07	51	7.84	33.60	1680	34.35	54.97
Time+Comfort_Level+Reliability	1354	38.63	59.07	272	13.24	37.85	54	14.81	36.26	1680	33.75	54.90
Price+Comfort_Level+Reliability	1355	41.03	60.17	269	11.90	37.06	56	12.50	36.78	1680	35.42	55.69
Time+Price+Comfort_Level+Reliability	1357	39.28	59.41	278	14.75	39.42	45	13.33	39.07	1680	34.52	55.56
Total_num	10669	40.32	59.23	2149	13.91	38.27	622	11.25	35.57	13440	34.76	54.79

Table 3. Ablation study on the model’s constraint understanding capability in Metromap and Travelmap scenarios. The experiment evaluates the calculation and understanding of constraints, including Total Time (T), Total Price (P), Average Comfort Level (C), and Average Reliability (R). “I” represents “Indicators”.

Metromap														
Constraint Settings	Qwen3-w/o I		Qwen3-four I						GPT4o-four I					
	EMA	PMA	EMA	PMA	T	P	C	R	EMA	PMA	T	P	C	R
Time-Only	19.81	39.47	19.00	36.10	0	2.44	2.88	9.69	41.13	59.61	0	12.06	7.62	19.00
Price-Only	22.06	42.40	19.19	37.11	0	1.19	4.06	10.44	38.00	58.47	0	13.44	5.06	16.31
Comfort_Level-Only	18.25	38.97	18.25	37.31	0	2.44	4.88	10.19	32.37	52.16	0	7.62	1.25	16.88
Reliability-Only	19.38	39.53	18.75	38.03	0	1.19	4.06	10.44	31.13	51.97	0	7.12	2.94	14.87
Time+Price+Reliability	19.25	38.91	19.25	37.09	0	2.19	3.87	9.81	37.44	56.99	0	9.75	5.63	16.13
Time+Comfort_Level+Reliability	19.13	39.04	19.19	36.79	0	2.00	4.88	10.19	35.94	55.81	0	10.81	5.31	17.44
Price+Comfort_Level+Reliability	19.44	40.18	18.37	37.28	0	1.75	4.31	11.00	34.88	55.75	0	10.00	4.06	15.81
Time+Price+Comfort_Level+Reliability	19.31	39.31	19.19	37.18	0	2.13	5.19	10.69	37.25	56.00	0	9.31	6.12	16.44

Travelmap														
Constraint Settings	Qwen3-w/o I		Qwen3-four I						GPT4o-four I					
	EMA	PMA	EMA	PMA	T	P	C	R	EMA	PMA	T	P	C	R
Time-Only	29.94	45.70	27.08	42.91	0	0.12	1.07	4.46	40.65	53.19	0.12	0.06	1.61	4.82
Price-Only	38.69	57.11	35.42	54.33	0.06	0.06	1.25	4.05	52.32	66.99	0.12	0.06	1.49	5.30
Comfort_Level-Only	34.17	56.28	33.51	54.33	0.12	0	1.43	5.00	42.68	62.30	0.24	0.18	0.60	4.76
Reliability-Only	37.20	58.08	34.35	54.82	0.06	0.06	1.19	3.87	35.06	58.38	0.06	0.06	1.19	1.96
Time+Price+Reliability	34.35	54.97	34.70	54.89	0.12	0.06	1.07	4.29	48.45	64.76	0.06	0.24	1.37	4.70
Time+Comfort_Level+Reliability	33.75	54.90	33.15	53.82	0.12	0.00	1.49	4.35	48.45	64.95	0.12	0.18	1.07	5.00
Price+Comfort_Level+Reliability	35.42	55.69	33.87	54.37	0.06	0.06	1.67	4.11	48.57	64.80	0.18	0.18	0.65	5.54
Time+Price+Comfort_Level+Reliability	34.52	55.56	33.21	53.97	0.06	0.18	1.49	4.82	48.27	64.71	0.06	0.06	1.13	5.65

Furthermore, as shown in Table 3, to examine the models’ understanding and computational ability regarding constraints, we require both Qwen3-VL-8B-Instruct and GPT-4o to output the constraint-related indicators, Total Time (T), Total Price (P), Average Comfort Level (C), and Average Reliability (R), for the optimal path in each task.

We analyze the results from the following four aspects:

Observation 1: “Shortest-path trap”. As shown in Table 2, high performance is concentrated in the FR category. In

the Metromap scenario, when the numbers of PR and NR samples are 957 and 2481 respectively, their effective planning ratios are only 0.73% and 2.74%. This suggests that models primarily depend on shortest-path guessing, succeeding only when the shortest path happens to meet the constraints, rather than truly understanding them.

Observation 2: Counting and numerical computation deficiencies. Table 3 shows that models struggle with numerical tasks like counting and computation. When asked

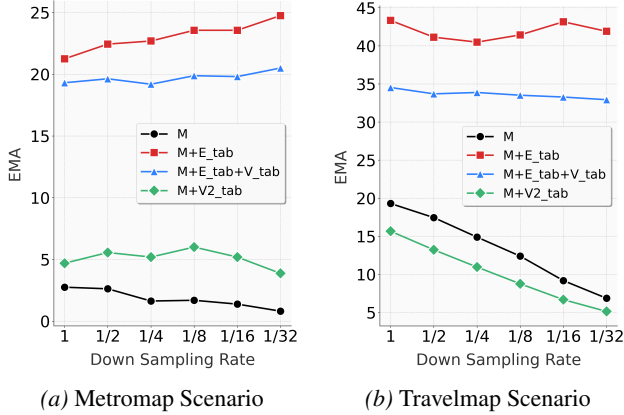


Figure 3. Impact of image resolution on Route Planning (RP) tasks in (a) Metromap and (b) Travelmap scenarios. Images are downsampled to ratios of 1/2, 1/4, 1/8, 1/16, and 1/32. Performance is evaluated under four map-based input settings: Map-Only (M), Map+Edge_{tab} (M+E_{tab}), Map+Edge_{tab}+Vertex_{tab} (M+E_{tab}+V_{tab}), and Map+Vertex₂_{tab} (M+V₂_{tab}).

to provide computed values, performance declines. QA experiments in Appendix F.2 show that, while the models exhibit cross-modal integration capabilities, they struggle with tasks such as station counting, numerical comparison, and multi-hop reasoning.

Observation 3: Heterogeneous graphs limited understanding. Results from Tables 2 and 3 both show that model performance drops to near 0 on weighted and heterogeneous graph tasks, with little improvement even under simplified constraints. This indicates that current models have difficulties in modeling weight relations, which are further amplified in heterogeneous graph settings.

Observation 4: Multi-step Reasoning Bottleneck. As shown in Table 2, all time-related indicators drop to zero once “transfer time” is introduced, revealing that models fail under even minimal multi-step reasoning complexity.

4.2.3. ABLATION STUDY OF RP FOR RESOLUTION

To analyze the effects of visual perception degradation across 2 task types, Figure 3 illustrates the impact of different image resolutions on RP task under two scenarios:

Metromap scenario. Under Map+Edge_{tab} and Map+E_{tab}+V_{tab}, image downsampling improves performance despite reduced visual fidelity, indicating that models primarily rely on E_{tab} while visual maps may introduce interference. Under Map+V_{tab}, performance remains largely stable, suggesting dependence on global graph information rather than local visual details. In contrast, in the Map-only setting, performance consistently degrades with downsampling, demonstrating that purely visual reasoning is highly sensitive to visual quality.

Travelmap scenario. Downsampling generally degrades

performance, but a rebound under the E_{tab} setting indicates that models initially attend to both visual and tabular inputs, but progressively shift their reasoning toward E_{tab} as image quality degrades. These results suggest that E_{tab} parsing defines the performance floor, whereas visual perception quality determines the performance ceiling. Thus, improving model’s performance ceiling is more fundamentally contingent upon the accurate perception and stable representation of crucial information in complex images.

4.2.4. OTHER EXPERIMENTAL RESULTS

The following summarizes the five groups of experimental results presented in the Appendix F:

- *QA task performance evaluation (Appendix F.2):* Models perform well on localization tasks, but struggle with counting, numerical computation, and multi-step reasoning tasks.
- *Analysis across different Map Difficulty and Query Difficulty levels (Appendix F.3):* Performance degradation patterns differ significantly as Map and Query Difficulty levels increase, particularly between Metromap and Travelmap.
- *Impact of image resolution on QA tasks (Appendix F.4):* Improvements in image clarity alone do not constitute a sufficient condition for enhancing model performance.
- *Impact of tabular modality formats on RP and QA tasks (Appendix F.5):* CSV format significantly reduces token overhead without inducing noticeable performance degradation.
- *Impact of language distribution on RP tasks (Appendix F.6):* Models perform better when the image language is high-frequency languages (e.g., Chinese or English), while differences in native language have a relatively limited impact on performance.

5. Conclusion

This study introduces **MapTab**, a multimodal benchmark for multi-constraint heterogeneous graph reasoning that jointly leverages *images and structured data*. Covering two real-world scenarios, *Metromap* and *Travelmap*, MapTab provides 328 de-redundant maps with multi-dimensional constraints in *Edge_{tab}* and *Vertex_{tab}*, generating 196,800 RP samples and 3,936 QA samples for comprehensive evaluation. Systematic testing of 15 state-of-the-art MLLMs reveals enduring challenges in dense visual perception, multimodal integration, constraint reasoning, and long-horizon numerical or multi-step tasks. As MapTab currently targets static topological graphs, these findings emphasize the importance of exploring dynamic

environments, more complex maps, and real-time reasoning in the future work.

Impact Statement

This paper presents work whose goal is to advance the field of Machine Learning. There are many potential societal consequences of our work, none which we feel must be specifically highlighted here.

References

- Abdin, M., Aneja, J., Awadalla, H., Awadallah, A., Awan, A. A., Bach, N., Bahree, A., Bakhtiari, A., Bao, J., Behl, H., Benhaim, A., Bilenko, M., Bjorck, J., Bubeck, S., Cai, M., Cai, Q., Chaudhary, V., Chen, D., Chen, D., Chen, W., Chen, Y.-C., Chen, Y.-L., Cheng, H., Chopra, P., Dai, X., Dixon, M., Eldan, R., Frago, V., Gao, J., Gao, M., Gao, M., Garg, A., Giorno, A. D., Goswami, A., Gunasekar, S., Haider, E., Hao, J., Hewett, R. J., Hu, W., Huynh, J., Iyer, D., Jacobs, S. A., Javaheripi, M., Jin, X., Karampatziakis, N., Kauffmann, P., Khademi, M., Kim, D., Kim, Y. J., Kurilenko, L., Lee, J. R., Lee, Y. T., Li, Y., Li, Y., Liang, C., Liden, L., Lin, X., Lin, Z., Liu, C., Liu, L., Liu, M., Liu, W., Liu, X., Luo, C., Madan, P., Mahmoudzadeh, A., Majercak, D., Mazzola, M., Mendes, C. C. T., Mitra, A., Modi, H., Nguyen, A., Norick, B., Patra, B., Perez-Becker, D., Portet, T., Pryzant, R., Qin, H., Radmilac, M., Ren, L., de Rosa, G., Rosset, C., Roy, S., Ruwase, O., Saarikivi, O., Saied, A., Salim, A., Santacrose, M., Shah, S., Shang, N., Sharma, H., Shen, Y., Shukla, S., Song, X., Tanaka, M., Tupini, A., Vaddamanu, P., Wang, C., Wang, G., Wang, L., Wang, S., Wang, X., Wang, Y., Ward, R., Wen, W., Witte, P., Wu, H., Wu, X., Wyatt, M., Xiao, B., Xu, C., Xu, J., Xu, W., Xue, J., Yadav, S., Yang, F., Yang, J., Yang, Y., Yang, Z., Yu, D., Yuan, L., Zhang, C., Zhang, C., Zhang, J., Zhang, L. L., Zhang, Y., Zhang, Y., Zhang, Y., and Zhou, X. Phi-3 technical report: A highly capable language model locally on your phone, 2024a. URL <https://arxiv.org/abs/2404.14219>.
- Abdin, M., Aneja, J., Behl, H., Bubeck, S., Eldan, R., Gunasekar, S., Harrison, M., Hewett, R. J., Javaheripi, M., Kauffmann, P., et al. Phi-4 technical report. *arXiv preprint arXiv:2412.08905*, 2024b.
- Achiam, J., Adler, S., Agarwal, S., Ahmad, L., Akkaya, I., Aleman, F. L., Almeida, D., Altenschmidt, J., Altman, S., Anadkat, S., et al. Gpt-4 technical report. *arXiv preprint arXiv:2303.08774*, 2023.
- Bai, S., Cai, Y., Chen, R., Chen, K., Chen, X., Cheng, Z., Deng, L., Ding, W., Gao, C., Ge, C., Ge, W., Guo, Z., Huang, Q., Huang, J., Huang, F., Hui, B., Jiang, S., Li, Z., Li, M., Li, M., Li, K., Lin, Z., Lin, J., Liu, X., Liu, J., Liu, C., Liu, Y., Liu, D., Liu, S., Lu, D., Luo, R., Lv, C., Men, R., Meng, L., Ren, X., Ren, X., Song, S., Sun, Y., Tang, J., Tu, J., Wan, J., Wang, P., Wang, P., Wang, Q., Wang, Y., Xie, T., Xu, Y., Xu, H., Xu, J., Yang, Z., Yang, M., Yang, J., Yang, A., Yu, B., Zhang, F., Zhang, H., Zhang, X., Zheng, B., Zhong, H., Zhou, J., Zhou, F., Zhou, J., Zhu, Y., and Zhu, K. Qwen3-vl technical report, 2025a. URL <https://arxiv.org/abs/2511.21631>.
- Bai, S., Chen, K., Liu, X., Wang, J., Ge, W., Song, S., Dang, K., Wang, P., Wang, S., Tang, J., et al. Qwen2.5-vl technical report. *arXiv preprint arXiv:2502.13923*, 2025b.
- ByteDance. doubao-seed-1.6-thinking. https://www.volcengine.com/docs/82379/1593702?utm_source=chatgpt.com&lang=zh, 2025.
- ByteDance Seed Team. Seed1.6: Tech introduction. https://seed.bytedance.com/en/seed1_6, June 2025. Model ID: doubao-seed-1-6-251015. Accessed: 2025-12-25.
- Cai, Z., Wang, Y., Sun, Q., Wang, R., Gu, C., Yin, W., Lin, Z., Yang, Z., Wei, C., Qian, O., et al. Holistic evaluation of multimodal llms on spatial intelligence. *arXiv preprint arXiv:2508.13142*, 2025.
- Cao, C., Zhu, H., Ren, Z., Choset, H., and Zhang, J. Representation granularity enables time-efficient autonomous exploration in large, complex worlds. *Science Robotics*, 8(80):eadf0970, 2023.
- Cao, X., Zhou, T., Ma, Y., Ye, W., Cui, C., Tang, K., Cao, Z., Liang, K., Wang, Z., Rehg, J. M., et al. Maplm: A real-world large-scale vision-language benchmark for map and traffic scene understanding. In *Proceedings of the IEEE/CVF conference on computer vision and pattern recognition*, pp. 21819–21830, 2024.
- Chen, Y. Path planning algorithm for logistics autonomous vehicles at cainiao stations based on multi-sensor data fusion. *PLoS One*, 20(5):e0321257, 2025.
- Cheng, J., Liu, Y., Zhang, X., Fei, Y., Hong, W., Lyu, R., Wang, W., Su, Z., Gu, X., Liu, X., et al. Glyph: Scaling context windows via visual-text compression. *arXiv preprint arXiv:2510.17800*, 2025.
- Chollet, F., Knoop, M., Kamradt, G., Landers, B., and Pinkard, H. Arc-agi-2: A new challenge for frontier ai reasoning systems. *arXiv preprint arXiv:2505.11831*, 2025.
- Cui, C., Ma, Y., Cao, X., Ye, W., Zhou, Y., Liang, K., Chen, J., Lu, J., Yang, Z., Liao, K.-D., et al. A survey on multimodal large language models for autonomous driving.

- In *Proceedings of the IEEE/CVF winter conference on applications of computer vision*, pp. 958–979, 2024.
- Dihan, M. L., Hassan, M. T., Parvez, M. T., Hasan, M. H., Alam, M. A., Cheema, M. A., Ali, M. E., and Parvez, M. R. Mapeval: A map-based evaluation of geospatial reasoning in foundation models. *arXiv preprint arXiv:2501.00316*, 2024.
- Fang, B., Yang, Z., and Di, X. Travellm: Could you plan my new public transit route in face of a network disruption? *arXiv preprint arXiv:2407.14926*, 2024.
- Feng, J., Zhang, J., Yan, J., Zhang, X., Ouyang, T., Liu, T., Du, Y., Guo, S., and Li, Y. Citybench: Evaluating the capabilities of large language model as world model. *arXiv e-prints*, pp. arXiv–2406, 2024.
- Feng, J., Zhang, J., Liu, T., Zhang, X., Ouyang, T., Yan, J., Du, Y., Guo, S., and Li, Y. Citybench: Evaluating the capabilities of large language models for urban tasks. In *Proceedings of the 31st ACM SIGKDD Conference on Knowledge Discovery and Data Mining V. 2*, pp. 5413–5424, 2025a.
- Feng, S., Fang, G., Ma, X., and Wang, X. Efficient reasoning models: A survey. *arXiv preprint arXiv:2504.10903*, 2025b.
- Feng, S., Tuo, K., Wang, S., Kong, L., Zhu, J., and Wang, H. Rewardmap: Tackling sparse rewards in fine-grained visual reasoning via multi-stage reinforcement learning. *arXiv preprint arXiv:2510.02240*, 2025c.
- Feng, S., Wang, S., Ouyang, S., Kong, L., Song, Z., Zhu, J., Wang, H., and Wang, X. Can mllms guide me home? a benchmark study on fine-grained visual reasoning from transit maps. *arXiv preprint arXiv:2505.18675*, 2025d.
- Fu, D., Li, X., Wen, L., Dou, M., Cai, P., Shi, B., and Qiao, Y. Drive like a human: Rethinking autonomous driving with large language models. In *2024 IEEE/CVF Winter Conference on Applications of Computer Vision Workshops (WACVW)*, pp. 910–919. IEEE, 2024.
- Google. Gemini 3 flash: Frontier intelligence built for speed. <https://blog.google/products-and-platforms/products/gemini/gemini-3-flash/>, December 2025. Model ID: gemini-3-flash-preview. Accessed: 2025-12-25.
- Guo, D., Yang, D., Zhang, H., Song, J., Zhang, R., Xu, R., Zhu, Q., Ma, S., Wang, P., Bi, X., et al. Deepseek-r1: Incentivizing reasoning capability in llms via reinforcement learning. *arXiv preprint arXiv:2501.12948*, 2025a.
- Guo, L., Li, Z., and Min, S. Enhanced natural language annotation and query for semantic mapping in visual slam using large language models. *Journal of Sustainability, Policy, and Practice*, 1(3):131–143, 2025b.
- Guo, M.-H., Xu, J., Zhang, Y., Song, J., Peng, H., Deng, Y.-X., Dong, X., Nakayama, K., Geng, Z., Wang, C., et al. R-bench: Graduate-level multi-disciplinary benchmarks for llm & mllm complex reasoning evaluation. *arXiv preprint arXiv:2505.02018*, 2025c.
- Hong, Y., Sun, R., Li, B., Yao, X., Wu, M., Chien, A., Yin, D., Wu, Y. N., Wang, Z. J., and Chang, K.-W. Embodied web agents: Bridging physical-digital realms for integrated agent intelligence. *arXiv preprint arXiv:2506.15677*, 2025.
- Hu, T., Liu, X., Wang, S., Zhu, Y., Liang, A., Kong, L., Zhao, G., Gong, Z., Cen, J., Huang, Z., et al. Vision-language-action models for autonomous driving: Past, present, and future. *arXiv preprint arXiv:2512.16760*, 2025.
- Hu, Y., Shi, W., Fu, X., Roth, D., Ostendorf, M., Zettlemoyer, L., Smith, N. A., and Krishna, R. Visual sketchpad: Sketching as a visual chain of thought for multimodal language models. *Advances in Neural Information Processing Systems*, 37:139348–139379, 2024.
- Huang, J., Chen, R., Li, Z., Gao, Z., He, X., Guo, Y., Gong, M., and Liu, T. Mllm-for3d: Adapting multimodal large language model for 3d reasoning segmentation. *arXiv preprint arXiv:2503.18135*, 2025.
- Hurst, A., Lerer, A., Goucher, A. P., Perelman, A., Ramesh, A., Clark, A., Ostrow, A., Welihinda, A., Hayes, A., Radford, A., et al. Gpt-4o system card. *arXiv preprint arXiv:2410.21276*, 2024.
- Krechetova, V. and Kochedykov, D. Geobenchx: Benchmarking llms in agent solving multistep geospatial tasks. In *Proceedings of the 1st ACM SIGSPATIAL International Workshop on Generative and Agentic AI for Multi-Modality Space-Time Intelligence*, pp. 27–35, 2025.
- Li, K., Tian, Y., Hu, Q., Luo, Z., Huang, Z., and Ma, J. Mmcode: Benchmarking multimodal large language models for code generation with visually rich programming problems. *arXiv preprint arXiv:2404.09486*, 2024.
- Li, M., Zhong, J., Chen, T., Lai, Y., and Psounis, K. Eeebench: A comprehensive multimodal electrical and electronics engineering benchmark. In *Proceedings of the Computer Vision and Pattern Recognition Conference*, pp. 13337–13349, 2025a.

- Li, Z., Grossman, M., Kulkarni, M., Chen, M., Chiang, Y.-Y., et al. Mapqa: Open-domain geospatial question answering on map data. *arXiv preprint arXiv:2503.07871*, 2025b.
- Liu, H., Li, C., Li, Y., and Lee, Y. J. Improved baselines with visual instruction tuning, 2023.
- Lu, H., Liu, Z., Jiang, G., Luo, Y., Chen, S., Zhang, Y., and Chen, Y.-C. Uniugp: Unifying understanding, generation, and planing for end-to-end autonomous driving. *arXiv preprint arXiv:2512.09864*, 2025a.
- Lu, P., Gong, R., Jiang, S., Qiu, L., Huang, S., Liang, X., and Zhu, S.-C. Inter-gps: Interpretable geometry problem solving with formal language and symbolic reasoning. *arXiv preprint arXiv:2105.04165*, 2021.
- Lu, P., Bansal, H., Xia, T., Liu, J., Li, C., Hajishirzi, H., Cheng, H., Chang, K.-W., Galley, M., and Gao, J. Mathvista: Evaluating mathematical reasoning of foundation models in visual contexts. *arXiv preprint arXiv:2310.02255*, 2023.
- Lu, S., Li, Y., Xia, Y., Hu, Y., Zhao, S., Ma, Y., Wei, Z., Li, Y., Duan, L., Zhao, J., et al. Ovis2. 5 technical report. *arXiv preprint arXiv:2508.11737*, 2025b.
- Lu, Y., Cao, J., Wu, Y., Li, B., Tang, L., Ji, Y., Wu, C., Wu, J., and Zhu, W. Rsvp: Reasoning segmentation via visual prompting and multi-modal chain-of-thought. *arXiv preprint arXiv:2506.04277*, 2025c.
- OpenAI. OpenAI o1. <https://openai.com/o1/>, 2024.
- OpenAI. Gpt-4.1 model card. <https://platform.openai.com/docs/models/gpt-4.1>, April 2025a. Released on April 14, 2025.
- OpenAI. OpenAI o3 and o4-mini System Card. <https://cdn.openai.com/pdf/2221c875-02dc-4789-800b-e7758f3722c1/o3-and-o4-mini-system-card.pdf>, 2025b.
- Peng, Z., Wang, W., Dong, L., Hao, Y., Huang, S., Ma, S., and Wei, F. Kosmos-2: Grounding multimodal large language models to the world. *arXiv preprint arXiv:2306.14824*, 2023.
- Pyo, J., Jiao, Y., Jung, D., Li, Z., Jang, L., Kirsanova, S., Kim, J., Lin, Y., Liu, Q., Xie, J., et al. Frieda: Benchmarking multi-step cartographic reasoning in vision-language models. *arXiv preprint arXiv:2512.08016*, 2025.
- Qi, Y., Zhao, H., Guo, Z., Ma, S., Chen, Z., Han, Y., Zhang, R., Lin, Z., Xin, S., Huang, Y., et al. Bear: Benchmarking and enhancing multimodal language models for atomic embodied capabilities. *arXiv preprint arXiv:2510.08759*, 2025.
- Qiao, R., Tan, Q., Dong, G., MinhuiWu, M., Sun, C., Song, X., Wang, J., Gongque, Z., Lei, S., Zhang, Y., et al. We-math: Does your large multimodal model achieve human-like mathematical reasoning? In *Proceedings of the 63rd Annual Meeting of the Association for Computational Linguistics (Volume 1: Long Papers)*, pp. 20023–20070, 2025a.
- Qiao, Y., Hong, H., Lyu, W., An, D., Zhang, S., Xie, Y., Wang, X., and Wu, Q. Navbench: Probing multimodal large language models for embodied navigation. *arXiv preprint arXiv:2506.01031*, 2025b.
- Ranga, J., PRASATH, A. A., Kumar, N., Naveenkumar, R., Vadar, P. S., and Fiaz, A. S. Urbandriveway: A decision-making framework for navigating urban autonomous vehicles in complex traffic systems. In *2025 8th International Conference on Trends in Electronics and Informatics (ICOEI)*, pp. 1575–1582. IEEE, 2025.
- Ren, Y., Tertikas, K., Maiti, S., Han, J., Zhang, T., Süsstrunk, S., and Kokkinos, F. Vgrp-bench: Visual grid reasoning puzzle benchmark for large vision-language models. *arXiv preprint arXiv:2503.23064*, 2025.
- Shang, T., Li, Z., Xu, P., Qiao, J., Chen, G., Ruan, Z., and Hu, W. Bridging text and vision: A multi-view text-vision registration approach for cross-modal place recognition. *arXiv preprint arXiv:2502.14195*, 2025.
- Shao, Z., Wang, P., Zhu, Q., Xu, R., Song, J., Bi, X., Zhang, H., Zhang, M., Li, Y., Wu, Y., et al. Deepseekmath: Pushing the limits of mathematical reasoning in open language models. *arXiv preprint arXiv:2402.03300*, 2024.
- Shoaib, M. R., Emara, H. M., and Zhao, J. A survey on the applications of frontier ai, foundation models, and large language models to intelligent transportation systems. In *2023 International Conference on Computer and Applications (ICCA)*, pp. 1–7. IEEE, 2023.
- Shridhar, M., Yuan, X., Côté, M.-A., Bisk, Y., Trischler, A., and Hausknecht, M. Alfworld: Aligning text and embodied environments for interactive learning. *arXiv preprint arXiv:2010.03768*, 2020.
- Sima, C., Renz, K., Chitta, K., Chen, L., Zhang, H., Xie, C., Beißwenger, J., Luo, P., Geiger, A., and Li, H. Drivelm: Driving with graph visual question answering. In *European conference on computer vision*, pp. 256–274. Springer, 2024.

- Song, Y., Ou, T., Kong, Y., Li, Z., Neubig, G., and Yue, X. Visualpuzzles: Decoupling multimodal reasoning evaluation from domain knowledge. *arXiv preprint arXiv:2504.10342*, 2025.
- Srivastava, V., Lei, F., Mukhopadhyay, S., Gupta, V., and Maciejewski, R. Mapiq: Evaluating multimodal large language models for map question answering. *arXiv preprint arXiv:2507.11625*, 2025.
- Tan, W., Jiang, C., Duan, Y., Lei, M., Li, J., Hong, Y., Wang, X., and An, B. Stardojo: Benchmarking open-ended behaviors of agentic multimodal llms in production-living simulations with stardew valley. *arXiv preprint arXiv:2507.07445*, 2025a.
- Tan, W., Li, X., Fang, Y., Yao, H., Yan, S., Luo, H., Ao, T., Li, H., Ren, H., Yi, B., et al. Lumine: An open recipe for building generalist agents in 3d open worlds. *arXiv preprint arXiv:2511.08892*, 2025b.
- Team, G., Anil, R., Borgeaud, S., Alayrac, J.-B., Yu, J., Soricut, R., Schalkwyk, J., Dai, A. M., Hauth, A., Millican, K., et al. Gemini: a family of highly capable multimodal models. *arXiv preprint arXiv:2312.11805*, 2023.
- Team, K., Du, A., Yin, B., Xing, B., Qu, B., Wang, B., Chen, C., Zhang, C., Du, C., Wei, C., et al. Kimi-vl technical report. *arXiv preprint arXiv:2504.07491*, 2025.
- Ung, H. Q., Habault, G., Nishimura, Y., Niu, H., Legaspi, R., Oya, T., Kojima, R., Taya, M., Ono, C., Minamikawa, A., et al. Cartomapqa: A fundamental benchmark dataset evaluating vision-language models on cartographic map understanding. In *Proceedings of the 33rd ACM International Conference on Advances in Geographic Information Systems*, pp. 440–453, 2025.
- Venu, S. and Gurusamy, M. A comprehensive review of path planning algorithms for autonomous navigation. *Results in Engineering*, pp. 107750, 2025.
- Wang, K., Pan, J., Shi, W., Lu, Z., Ren, H., Zhou, A., Zhan, M., and Li, H. Measuring multimodal mathematical reasoning with math-vision dataset. *Advances in Neural Information Processing Systems*, 37:95095–95169, 2024a.
- Wang, W., Di, X., Liu, M., and Gao, F. Multi-level symmetric semantic alignment network for image–text matching. *Neurocomputing*, 599:128082, 2024b.
- Wang, Z., Li, X., Ye, Y., Fang, J., Wang, H., Liu, L., Liang, S., Lu, J., Wu, Z., Feng, J., et al. Game-tars: Pre-trained foundation models for scalable generalist multimodal game agents. *arXiv preprint arXiv:2510.23691*, 2025.
- Wen, L., Fu, D., Li, X., Cai, X., Ma, T., Cai, P., Dou, M., Shi, B., He, L., and Qiao, Y. Dilu: A knowledge-driven approach to autonomous driving with large language models. *arXiv preprint arXiv:2309.16292*, 2023.
- Wong, L. H. K., Kang, X., Bai, K., and Zhang, J. A survey of robotic navigation and manipulation with physics simulators in the era of embodied ai. *arXiv preprint arXiv:2505.01458*, 2025.
- Wu, H., Huang, X., Chen, Y., Zhang, Y., Wang, Y., and Xie, W. Spatialscore: Towards unified evaluation for multimodal spatial understanding. *arXiv preprint arXiv:2505.17012*, 2025.
- Wu, P. and Xie, S. V*: Guided visual search as a core mechanism in multimodal llms. In *Proceedings of the IEEE/CVF Conference on Computer Vision and Pattern Recognition*, pp. 13084–13094, 2024.
- Wu, Z., Chen, X., Pan, Z., Liu, X., Liu, W., Dai, D., Gao, H., Ma, Y., Wu, C., Wang, B., et al. Deepseek-vl2: Mixture-of-experts vision-language models for advanced multimodal understanding. *arXiv preprint arXiv:2412.10302*, 2024.
- Xiao, Y., Sun, E., Liu, T., and Wang, W. Logicvista: Multimodal llm logical reasoning benchmark in visual contexts. *arXiv preprint arXiv:2407.04973*, 2024.
- Xie, S., Kong, L., Dong, Y., Sima, C., Zhang, W., Chen, Q. A., Liu, Z., and Pan, L. Are vlms ready for autonomous driving? an empirical study from the reliability, data, and metric perspectives. *arXiv preprint arXiv:2501.04003*, 2025.
- Xing, S., Sun, Z., Xie, S., Chen, K., Huang, Y., Wang, Y., Li, J., Song, D., and Tu, Z. Can large vision language models read maps like a human? *arXiv preprint arXiv:2503.14607*, 2025.
- Xu, H., Hu, Y., Gao, C., Zhu, Z., Zhao, Y., Li, Y., and Yin, Q. Geonav: Empowering mllms with explicit geospatial reasoning abilities for language-goal aerial navigation. *arXiv preprint arXiv:2504.09587*, 2025a.
- Xu, W., Wang, J., Wang, W., Chen, Z., Zhou, W., Yang, A., Lu, L., Li, H., Wang, X., Zhu, X., et al. Visulogic: A benchmark for evaluating visual reasoning in multi-modal large language models. *arXiv preprint arXiv:2504.15279*, 2025b.
- Xu, Y., Pan, Y., Liu, Z., and Wang, H. Flame: Learning to navigate with multimodal llm in urban environments. In *Proceedings of the AAAI Conference on Artificial Intelligence*, volume 39, pp. 9005–9013, 2025c.

- Yan, H. and Lv, Z. A survey of sustainable development of intelligent transportation system based on urban travel demand. *Development*, 2(1):2399, 2024.
- Yang, J., Yang, S., Gupta, A. W., Han, R., Fei-Fei, L., and Xie, S. Thinking in space: How multimodal large language models see, remember, and recall spaces. In *Proceedings of the Computer Vision and Pattern Recognition Conference*, pp. 10632–10643, 2025a.
- Yang, R., Chen, H., Zhang, J., Zhao, M., Qian, C., Wang, K., Wang, Q., Koripella, T. V., Movahedi, M., Li, M., et al. Embodiedbench: Comprehensive benchmarking multi-modal large language models for vision-driven embodied agents. *arXiv preprint arXiv:2502.09560*, 2025b.
- Yang, Z., Chen, J., Du, Z., Yu, W., Wang, W., Hong, W., Jiang, Z., Xu, B., and Tang, J. Mathglm-vision: solving mathematical problems with multi-modal large language model. *arXiv preprint arXiv:2409.13729*, 2024.
- Yao, J., Yang, S., Xu, J., Hu, L., Li, M., and Wang, D. Understanding the repeat curse in large language models from a feature perspective. *arXiv preprint arXiv:2504.14218*, 2025.
- Yarom, M., Bitton, Y., Changpinyo, S., Aharoni, R., Herzig, J., Lang, O., Ofek, E., and Szepes, I. What you see is what you read? improving text-image alignment evaluation. *Advances in Neural Information Processing Systems*, 36:1601–1619, 2023.
- Yu, R., Ma, X., and Wang, X. Introducing visual perception token into multimodal large language model. *arXiv preprint arXiv:2502.17425*, 2025.
- Yuan, F., Yan, Y., Jiang, Y., Zhao, H., Feng, T., Chen, J., Lou, Y., Zhang, W., Shen, Y., Lu, W., et al. Gsm8k-v: Can vision language models solve grade school math word problems in visual contexts. *arXiv preprint arXiv:2509.25160*, 2025.
- Yue, X., Ni, Y., Zhang, K., Zheng, T., Liu, R., Zhang, G., Stevens, S., Jiang, D., Ren, W., Sun, Y., et al. Mmmu: A massive multi-discipline multimodal understanding and reasoning benchmark for expert agi. In *Proceedings of the IEEE/CVF Conference on Computer Vision and Pattern Recognition*, pp. 9556–9567, 2024.
- Yue, X., Sun, J., Lu, J., Yao, L., Xia, F., Wang, T., Rao, F., Lyu, J., and Deng, Y. Instruction-augmented multimodal alignment for image-text and element matching. In *Proceedings of the Computer Vision and Pattern Recognition Conference*, pp. 1379–1388, 2025.
- Zeng, Q., Yang, Q., Dong, S., Du, H., Zheng, L., Xu, F., and Li, Y. Perceive, reflect, and plan: Designing llm agent for goal-directed city navigation without instructions. *arXiv preprint arXiv:2408.04168*, 2024.
- Zhang, K. Openmaskdino3d: Reasoning 3d segmentation via large language model. *arXiv preprint arXiv:2506.04837*, 2025.
- Zhang, R., Jiang, D., Zhang, Y., Lin, H., Guo, Z., Qiu, P., Zhou, A., Lu, P., Chang, K.-W., Qiao, Y., et al. Mathverse: Does your multi-modal llm truly see the diagrams in visual math problems? In *European Conference on Computer Vision*, pp. 169–186. Springer, 2024.
- Zhang, Y.-F., Lu, X., Yin, S., Fu, C., Chen, W., Hu, X., Wen, B., Jiang, K., Liu, C., Zhang, T., et al. Thyme: Think beyond images. *arXiv preprint arXiv:2508.11630*, 2025.
- Zheng, Y., Xing, Z., Zhang, Q., Jin, B., Li, P., Zheng, Y., Xia, Z., Zhan, K., Lang, X., Chen, Y., et al. Planagent: A multi-modal large language agent for closed-loop vehicle motion planning. *arXiv preprint arXiv:2406.01587*, 2024.
- Zheng, Y., Ying, J., Duan, H., Li, C., Zhang, Z., Liu, J., Liu, X., and Zhai, G. Geox-bench: Benchmarking cross-view geo-localization and pose estimation capabilities of large multimodal models. *arXiv preprint arXiv:2511.13259*, 2025a.
- Zheng, Z., Yang, M., Hong, J., Zhao, C., Xu, G., Yang, L., Shen, C., and Yu, X. Deepeyes: Incentivizing "thinking with images" via reinforcement learning. *arXiv preprint arXiv:2505.14362*, 2025b.
- Zhou, X., Wen, Y., Shao, Z., Li, W., Li, K., Li, H., Xie, X., and Yan, Z. Cartomark: a benchmark dataset for map pattern recognition and map content retrieval with machine intelligence. *Scientific Data*, 11(1):1205, 2024.
- Zhu, J., Wang, W., Chen, Z., Liu, Z., Ye, S., Gu, L., Tian, H., Duan, Y., Su, W., Shao, J., et al. Internvl3: Exploring advanced training and test-time recipes for open-source multimodal models. *arXiv preprint arXiv:2504.10479*, 2025.

Table of Contents in Appendix

A	Related Works	15
A.1.	Reasoning Abilities in LLMs and MLLMs	15
A.2.	Multimodal Reasoning Benchmarks	15
A.3.	Map-Based Spatial Reasoning and Planning	16
B	More Details for Dataset Construction	16
B.1.	QA Queries Construction	16
B.2.	RP Query Distribution Based on Difficulty Metrics	17
B.3.	Quality Control: Metromap Validation Algorithm	19
B.4.	Quality Control: Travelmap Validation Algorithm	19
C	Metrics	19
C.1.	Performance Metrics	19
C.2.	Difficulty Classification Metrics	20
D	Query Template	21
D.1.	RP Query	21
D.2.	QA Query	22
E	Prompt Template	24
E.1.	Prompts for Generating Edge_tab and Vertex_tab	24
E.2.	Prompts for RP Queries	29
E.3.	Prompts for QA Queries	34
F	More Experiments	36
F.1.	Experimental Settings	36
F.2.	Performance of MLLMs on QA	37
F.3.	Ablation study of Map & Query difficulty	40
F.4.	Ablation study of QA for resolution	41
F.5.	Ablation study of Tabular Modality	42
F.6.	Ablation study of Language	42
G	Error Case Analysis	43
H	Limitations	44

A. Related Works

A.1. Reasoning Abilities in LLMs and MLLMs

The rapid rise of multimodal large language models (MLLMs) (Bai et al., 2025a;b; Zhu et al., 2025; Abdin et al., 2024b; Hurst et al., 2024; Team et al., 2023) has fundamentally reshaped vision-language interaction, which have demonstrated strong capabilities in visual grounding (Peng et al., 2023; Shang et al., 2025; Guo et al., 2025b), reasoning-based segmentation (Huang et al., 2025; Lu et al., 2025c; Zhang, 2025), and text-image alignment (Yue et al., 2025; Wang et al., 2024b; Yarom et al., 2023).

Recently, the integration of reinforcement learning (RL) fine-tuning paradigms (Zhang et al., 2025; Zheng et al., 2025b; Feng et al., 2025b) has significantly expanded the reasoning capabilities of large language models (LLMs) (Guo et al., 2025a). Methods such as Group Relative Policy Optimization (GRPO) (Shao et al., 2024) have been particularly effective in activating and enhancing the latent logical deduction abilities within these models. These advancements have enabled LLMs to achieve improved performance in complex reasoning tasks, including mathematical reasoning (Yuan et al., 2025; Yang et al., 2024; Wang et al., 2024a), fine-grained spatial understanding (Wu et al., 2025; Yang et al., 2025a; Cai et al., 2025), and logical reasoning (Xu et al., 2025b; Xiao et al., 2024; Chollet et al., 2025).

Furthermore, the introduction of visual chain-of-thought and multi-dimensional perception has significantly enhanced multimodal reasoning in LLMs (OpenAI, 2024; 2025b; ByteDance, 2025; Team et al., 2025) and multimodal large language models (MLLMs), allowing them to integrate and reason across both visual and textual modalities. These models' improved reasoning capabilities have broad implications for real-world applications, including embodied intelligence (Hong et al., 2025; Qi et al., 2025; Yang et al., 2025b; Shridhar et al., 2020), game agents (Tan et al., 2025b; Wang et al., 2025; Tan et al., 2025a), and autonomous driving (Cui et al., 2024; Hu et al., 2025; Lu et al., 2025a), where sophisticated reasoning is required to make complex decisions in dynamic, multimodal environments.

Against this backdrop, a series of reasoning-oriented multimodal large language models (MLLMs) that inherit advantages from earlier architectural designs have emerged (Bai et al., 2025a;b; Zhu et al., 2025; Abdin et al., 2024b; Achiam et al., 2023; Team et al., 2023). Among them, models such as OpenAI 4o (Hurst et al., 2024), Gemini (Team et al., 2023), and Qwen (Bai et al., 2025a) have become key reference points for measuring the current level of cross-modal intelligence.

A.2. Multimodal Reasoning Benchmarks

Along with the rapid evolution of model capabilities, constructing multidimensional and interpretable evaluation frameworks to systematically characterize the performance of MLLMs across different reasoning levels has become a central challenge in the field (Lu et al., 2023; Qiao et al., 2025a; Li et al., 2024; Lu et al., 2021; Li et al., 2025a). Early benchmarks, including V*Bench (Wu & Xie, 2024), VisualPuzzles (Song et al., 2025), VisuLogic (Xu et al., 2025b), R-Bench (Guo et al., 2025c), and VGRP-Bench (Ren et al., 2025), primarily relied on synthetic tasks to assess abstract reasoning abilities related to logical structure construction and pattern recognition. Subsequently, benchmarks such as MathVQA (Wang et al., 2024a), MMMU (Yue et al., 2024), and MathVerse (Zhang et al., 2024) further introduced cross-modal mathematical reasoning to examine model performance under scenarios requiring deep integration of symbolic and visual information. Moreover, CityBench (Feng et al., 2025a) and DriveBench (Xie et al., 2025) *et al.* further extended evaluation to spatial reasoning in urban scenarios.

As an important carrier of high-density geospatial information, map-based visual question answering has gradually evolved into a key research direction for evaluating the depth of multimodal cognition. In this context, MapEval (Dihan et al., 2024), MapQA (Li et al., 2025b), MapIQ (Srivastava et al., 2025), and CartoMark (Zhou et al., 2024) have systematically revealed, from perspectives ranging from holistic evaluation and basic perception to textual element parsing, the substantial gap between multimodal models and human performance in geospatial cognition, as well as shared limitations in perception-reasoning decoupling and fine-grained semantic understanding.

Furthermore, at the level of higher-order spatial reasoning, FRIEDA (Pyo et al., 2025) and GeoX-Bench (Zheng et al., 2025a) expose structural deficiencies in complex spatial orientation and compositional reasoning, while CartoMapQA (Ung et al., 2025), through hierarchical evaluation in real-world map service scenarios, characterizes reasoning bottlenecks in practical tasks such as scale understanding and route navigation.

However, although existing benchmarks are able to uncover deficiencies in local perception and specific spatial tasks, their overall coverage of model capabilities remains limited. Most evaluations focus on visual question answering and local

perceptual skills, while lacking systematic characterization of global spatial modeling, long-range dependency reasoning, and sequential decision-making. Moreover, existing datasets generally fail to explicitly incorporate multidimensional real-world constraints and user-specific demands, making it difficult to comprehensively reflect the upper bounds of large models’ reasoning and decision-making capabilities in realistic and complex scenarios.

A.3. Map-Based Spatial Reasoning and Planning

In multimodal reasoning research, map-based spatial reasoning and planning have become core problems in navigation (Wong et al., 2025; Venu & Gurusamy, 2025; Xu et al., 2025c; Ranga et al., 2025), intelligent transportation (Shoaib et al., 2023; Yan & Lv, 2024; Chen, 2025), and autonomous driving (Fu et al., 2024; Wen et al., 2023; Sima et al., 2024). Compared with traditional perception-driven map understanding tasks, these studies place greater emphasis on a model’s ability to jointly model spatial structures, topological relationships, and long-tracing decision-making.

Recent works such as CityBench (Feng et al., 2024) and MapLM (Cao et al., 2024) explore map-driven spatial reasoning capabilities from different application scenarios, particularly examining model performance in transportation environments and urban contexts. Meanwhile, for embodied navigation tasks, researchers have proposed evaluation frameworks such as PlanAgent (Zheng et al., 2024), PReP (Zeng et al., 2024), GeoNav (Xu et al., 2025a), and NavBench (Qiao et al., 2025b). These frameworks assess the spatial reasoning capabilities of multimodal models from two complementary aspects: navigation understanding and step-by-step execution, thereby promoting a transition from static comprehension to dynamic action generation.

Although several benchmarks have focused on evaluating models’ reasoning and tool-use capabilities in multi-step spatial tasks, for example, GeoBenchX (Krechetova & Kochedykov, 2025), which examines collaborative reasoning through the integration of multiple geographic functions, and MapBench (Xing et al., 2025), which investigates hierarchical reading and attention mechanisms for multi-scale map information from a cognitive science perspective. Other benchmarks such as ReasonMap (Feng et al., 2025d), RewardMap (Feng et al., 2025c), and TravelLM (Fang et al., 2024) further evaluate autonomous reasoning and decision-making in complex scenarios by incorporating long-tracing logical reasoning, reinforcement learning feedback, and dynamic perturbation settings.

Nevertheless, despite examining spatial reasoning from multiple dimensions, these benchmarks generally overlook real-world constraints such as time, cost, and comfort, and often rely heavily on external tools, preventing a thorough evaluation of models’ pure visual reasoning capabilities.

In summary, existing RP-based benchmarks exhibit clear limitations in data scale and task complexity. Most fail to adequately consider multidimensional constraints present in real-world scenarios and struggle to effectively isolate model prior biases. Therefore, there is an urgent need for an evaluation framework that can eliminate prior interference while faithfully reflecting complex constraints and user demands, in order to comprehensively assess the integrated reasoning and decision-making capabilities of MLLMs.

B. More Details for Dataset Construction

B.1. QA Queries Construction

In MapTab, we design 24 types of QA tasks for both the Metromap and Travelmap scenarios, covering three dimensions: *Global Perception-based Reasoning*, *Local Perception-based Reasoning*, and *Spatial Relationship Judgment*. The experiments systematically configure four input modalities: *Map-only*, *Edge_tab-only*, *Vertex_tab-only*, and *Map+Vertex_tab*. The introduction of pure tabular modalities (Edge/Vertex-only) fills a gap in existing benchmarks regarding multimodal evaluation with *image + structured data*.

In particular, for the joint image-table input design in the Metromap scenario, we construct a strict *Cross-modal Necessity* setting by removing the *Line* column. By deliberately eliminating explicit topological cues, we create an *information gap* that forces models to deeply align and fuse visual features from high-resolution maps with semantic information from long-context tables, thereby authentically evaluating multimodal joint reasoning capabilities under single-modality deficiency.

To eliminate instruction bias and enhance evaluation robustness, each QA task category is equipped with five semantically equivalent but stylistically distinct instruction templates. These templates span diverse expression styles, including Direct / Neutral, Simple & Conversational, Slightly Formal, Technical / Academic Style, and Concise / Dataset-Friendly, and are cyclically applied during question generation. Detailed question examples are provided in Appendix D.2.

As shown in Appendix D.2, all QA tasks in this study are strictly limited to binary judgment questions and multiple-choice questions. During answer generation, we adopt a dual-track strategy. For tasks that can be logically derived from Edge_tab and Vertex_tab, ground-truth answers are automatically generated using Python scripts. For more complex tasks that cannot be fully covered by rule-based logic, the Gemini-3-Flash (Google, 2025) model is invoked for reasoning-based answer generation.

During model inference, we apply a structured extraction scheme that precisely captures predictions between two tags $\langle \text{answer_begin} \rangle$ and $\langle \text{answer_end} \rangle$. To ensure absolute rigor of the benchmark data, all model-generated preliminary answers are subsequently verified and validated through manual inspection.

B.2. RP Query Distribution Based on Difficulty Classification Metrics

To achieve fair and balanced allocation of query numbers for Metromap and Travelmap across training and test sets, we propose the following distribution strategy:

- 1. Input and target definition:** Given a set of cities/attractions \mathcal{C} , total query number Q , weighting exponent α , and minimum query threshold Q_{\min} , the algorithm takes these parameters as input and outputs the query number q_c for each city/attraction.
- 2. Difficulty grouping and target initialization (Phase 1):** Based on the Map Difficulty labels (Hard, Medium, Easy), cities/attractions are divided into three groups G_{Easy} , G_{Medium} , and G_{Hard} . The base query number is set as $\text{base} = \lfloor Q/3 \rfloor$. The target query numbers for the Medium and Hard groups, T_{Medium} and T_{Hard} , are both initialized to this base value, while the remaining queries are assigned to the Easy group as $T_{\text{Easy}} = Q - 2 \times \text{base}$, ensuring conservation of the total query count.
- 3. Training and test target allocation:** Within each difficulty group, cities/attractions are first separated according to image set type labels (training_set or test_set). Target query numbers $\text{target}_{\text{train}}$ and $\text{target}_{\text{test}}$ are then assigned to ensure a 4:1 ratio between training and test queries. This ratio applies to query counts rather than image counts (the image ratio is 2:1).
- 4. Intra-group weighted allocation (Phase 2):** Within each difficulty group and split (six groups in total), intra-group weights are computed based on the α -th power of each city’s/attraction’s Vertex Numbers. The total group weight is

$$W = \sum_{c \in S} (c.\text{Vertex Numbers})^\alpha.$$

Queries q_c are then allocated proportionally to ensure consistency with these weights.

- 5. Rounding and minimum threshold constraint:** Within each group, all cities/attractions except the last one apply rounding and enforce the minimum threshold Q_{\min} . The last city/attraction absorbs rounding errors to ensure that the group’s total query count exactly matches target_s . This city is recorded as $\text{LastCity}_{d,s}$ for later compensation.
- 6. Global ratio compensation (Phase 3):** After intra-group allocation, the total number of test queries is checked against the global target of 20% (i.e., $0.2Q$). If an excess $E > 0$ exists, queries are preferentially deducted from the last city/attraction in the Easy-test group ($\text{LastCity}_{\text{Easy},\text{test}}$) and evenly compensated to the last cities/attractions in the Medium-training and Hard-training groups ($\text{LastCity}_{d,\text{train}}$).
- 7. Minimum threshold consistency check:** After compensation, the adjusted last cities/attractions are checked to ensure their query counts do not fall below Q_{\min} . If violations occur, the second-to-last city/attraction is introduced into the compensation process, guaranteeing strict enforcement of the minimum threshold while maintaining the 4:1 training-test query ratio.

This algorithm is applicable to both Metromap and Travelmap. Taking Metromap as an example, the full algorithmic workflow is illustrated as Algorithm 1.

In the concrete setup, the total query numbers are set to $Q = 8000$ for Metromap and $Q = 8400$ for Travelmap. The intra-group weighting exponent is fixed to $\alpha = 1.5$, and the minimum query threshold is uniformly set to $Q_{\min} = 5$.

Algorithm 1 Balanced City Query Distribution Strategy

Input: City Data \mathcal{C} , Total Queries Q , Exponent α , Min Threshold Q_{\min}
Output: Query Numbers q_c for each city c
// Phase 1: Grouping and Target Initialization
Partition \mathcal{C} into $G_{\text{Easy}}, G_{\text{Medium}}, G_{\text{Hard}}$ based on Map Difficulty.
Set $base = \lfloor Q/3 \rfloor$.
Set $T_{\text{Medium}} = base, T_{\text{Hard}} = base, T_{\text{Easy}} = Q - 2 \times base$.
// Phase 2: Weighted Distribution per Group
for each difficulty $d \in \{\text{Easy}, \text{Medium}, \text{Hard}\}$ **do**
 Set $target_{\text{train}} = \lfloor T_d \times 0.8 \rfloor$ and $target_{\text{test}} = T_d - target_{\text{train}}$.
 for each subset type $s \in \{\text{train}, \text{test}\}$ **do**
 Let S be the set of cities in G_d of type s .
 Calculate weight sum $W = \sum_{c \in S} (c.\text{Vertex Numbers})^\alpha$.
 Initialize $assigned = 0$.
 for each city c in S **do**
 if c is not the last city **then**
 $raw_q = (c.\text{Vertex Numbers})^\alpha / W \times target_s$
 $q_c = \max(\text{round}(raw_q), Q_{\min})$
 else
 $q_c = target_s - assigned$ {Handle rounding remainder}
 Record c as $LastCity_{d,s}$ for potential compensation.
 end if
 $assigned = assigned + q_c$
 end for
 end for
// Phase 3: Global Ratio Compensation (Strict 4:1)
Calculate test excess $E = \sum_{c \in \text{Test}} q_c - (Q \times 0.2)$.
if $E > 0$ **then**
 // Step A: Reduce excess from Easy-Test
 Let $u = LastCity_{\text{Easy}, \text{test}}$.
 Update $q_u = q_u - E$.
 // Step B: Distribute excess to Medium/Hard Training
 Set $add_amt = E/2$.
 for $d \in \{\text{Medium}, \text{Hard}\}$ **do**
 Let $v = LastCity_{d, \text{train}}$.
 if $q_v + add_amt < Q_{\min}$ **then**
 Let v be the penultimate city in $G_d.\text{train}$.
 end if
 Update $q_v = q_v + add_amt$.
 end for
end if

The significance of this algorithm lies in achieving fair and balanced query allocation across multi-city/multi-attraction and multi-difficulty experimental settings. It prevents large cities/attractions from monopolizing query resources while ensuring sufficient data support for smaller ones, strictly maintains training-test ratios, and preserves reasonable data distributions, thereby guaranteeing sufficient model training and reliable evaluation. Moreover, the allocation results are traceable and controllable, ensuring that each city/attraction meets the minimum query threshold and providing a stable, interpretable, and reliable data foundation for multi-city/multi-attraction experiments.

B.3. Quality Control: Metromap Validation Algorithm

This section introduces a Metromap-specific validation algorithm designed to ensure the accuracy and consistency of metro line data in Edge_tab and Vertex_tab. The algorithm includes duplicate detection, station category comparison, vertex & edge cross-validation, transfer station annotation verification, and manual inspection, comprehensively identifying potential annotation errors and data inconsistencies:

1. **Duplicate detection:** First, edges in Edge_tab and stations in Vertex_tab are checked for duplication within the same metro line (Line). Specifically, if station A-B and B-A both appear, they are treated as the same edge. This step ensures the absence of redundant or duplicated metro information and verifies graph correctness.
2. **Station category set comparison:** Station categories in Edge_tab and Vertex_tab are collected and compared. This process checks for category consistency across the two files and helps identify annotation errors, especially when vertex and edge errors occur in different files.
3. **Vertex & edge cross-validation:** Based on the relationship between Edge_tab and Vertex_tab, the validation computes: $(\text{total number of edges in Edge_tab}) + (\text{number of metro line categories}) - (\text{number of loop lines})$, which should equal the total number of station occurrences in Vertex_tab. Ordinary stations are counted once, while transfer stations are counted according to the number of lines they belong to. This method detects cases where both Edge_tab and Vertex_tab contain errors that escape conventional validation.
4. **Transfer station annotation verification:** Transfer stations are checked separately in Edge_tab and Vertex_tab by expanding the set of lines each transfer station belongs to and comparing consistency across the two files. Transfer station identification criteria are defined as follows:
 - **Edge_tab:** if the same station name appears on multiple metro lines.
 - **Vertex_tab:** if a station’s Line column contains multiple lines or the Transfer Time value is greater than zero.
 - **Loop line identification:** in Edge_tab, if the first and last stations of the same line are identical, the line is considered a loop line. This step ensures accurate transfer station annotation and avoids errors arising from loop line special cases.
5. **Manual verification:** Finally, Edge_tab and Vertex_tab are manually checked against real metro maps to identify errors not detectable through automated validation.

B.4. Quality Control: Travelmap Validation Algorithm

The Travelmap-specific validation algorithm retains steps 1, 2, and 5 from the Metromap validation algorithm, with appropriate modifications to step 2. For Travelmap, Vertex_tab removes points that are completely disconnected from all others, retaining only connected vertices. In addition, Edge_tab is required to contain a single fully connected graph, preventing the existence of multiple disconnected subgraphs.

C. Metrics

This section proposes a unified evaluation framework designed to systematically assess model performance, map structural complexity, and query difficulty.

C.1. Performance Metrics

For model performance evaluation, the RP task adopts three core metrics Exact Match Accuracy (EMA), Partial Match Accuracy (PMA), and Difficulty-aware Score (DS) to comprehensively measure model performance in terms of path correctness, linguistic consistency, and format compliance. Given that the output format is strictly constrained by prompts, any result that does not conform to the required format is regarded as incorrect. Such format generation failures themselves indicate deficiencies in the model’s instruction understanding and execution capabilities. For QA tasks, evaluation is conducted solely based on Accuracy (Acc).

We first describe the performance metrics for the RP task in detail:

1. Exact Match Accuracy (EMA)

A score of 1 is assigned if the path generated by the model exactly matches the reference path in both station order and content; otherwise, a score of 0 is assigned. To tolerate minor spelling errors, a generated station name is considered identical to the reference station if the string similarity exceeds 50%. The similarity is computed based on character sequence matching, ignoring case differences and leading or trailing whitespaces. For Metromap, stations involving transfers must be explicitly annotated with the suffix “transfer”; otherwise, the station is considered incorrect. This transfer annotation requirement does not apply to Travelmap.

2. Partial Match Accuracy (PMA)

PMA measures the length of the longest contiguous correct prefix in the generated path, starting from the origin. Evaluation is conducted at the station level, counting only the continuously matched prefix until the first mismatched station appears (excluding the mismatched station). The PMA score is computed as the ratio of the length of this correct prefix to the total length of the reference path. This metric is preferred over simply measuring the proportion of correctly repeated stations, as we assume that once an error occurs in the path, subsequent planning steps become invalid and no longer reflect meaningful routing decisions.

3. Difficulty-aware Score (DS)

DS explicitly incorporates task difficulty into the evaluation. Each sample is assigned a discrete score ranging from 2 to 6 based on the combination of its Map_difficulty and Query_difficulty, denoted as Map_difficulty-Query_difficulty. Specifically, Easy, Medium, and Hard correspond to scores of 1, 2, and 3, respectively, and the final difficulty score is obtained by summing the two values. The difficulty score is counted only when EMA equals 1. This metric effectively reflects the upper bound of model performance, particularly its capability in handling high-difficulty tasks.

For QA-query tasks, all questions are either binary (true/false) or fill-in-the-blank. Evaluation is conducted using Accuracy (Acc): a score of 1 is assigned if the model-generated answer exactly matches the reference answer; otherwise, a score of 0 is assigned.

C.2. Difficulty Classification Metrics

This section introduces the classification methods for Map Difficulty and Query Difficulty. The core idea is to sort each Map and Query based on defined evaluation metrics and divide them into three levels: Hard, Medium, and Easy, with a ratio of 1:1:1. In Map Difficulty Classification, three indicators are considered: Graph Size (GS), Weighted Average Shortest Path (WASP), and Meshedness Coefficient (MC). In Query Difficulty Classification, addressing the specific scenarios of Metromap and Travelmap, the Shortest Path Length Index (SPLI) and Simple Path Complexity Index (SPCI) are adopted as difficulty metrics, respectively. These metrics comprehensively evaluate the complexity of Maps and Queries in RP tasks.

C.2.1. MAP DIFFICULTY CLASSIFICATION

1. Graph Size (GS)

Graph Size represents the overall “scale” of the graph, i.e., the sum of the number of nodes and edges:

$$GS = |V| + |E| \quad (2)$$

where $|V|$ denotes the number of nodes in the graph, and $|E|$ denotes the number of edges. This formula indicates that the size of the graph is equal to the sum of all nodes and edges, used to measure the complexity or overall volume of the graph.

2. Weighted Average Shortest Path (WASP)

WASP measures the average shortest path length between nodes in the graph, while considering the potential existence of multiple connected components. Let graph G have k connected components C_1, C_2, \dots, C_k , where the number of nodes in each connected component is $V_i = |C_i|$, and the shortest path length between nodes is $d(u, v)$. The unified expression is:

$$WASP = \frac{\sum_{i=1}^k |C_i| \cdot ASPD(C_i)}{\sum_{i=1}^k |C_i|} = \frac{\sum_{i=1}^k |C_i| \cdot ASPD(C_i)}{|V|} \quad (3)$$

Here, the inner summation and $ASPD(C_i)$ are used to calculate the average shortest path length of node pairs within each connected component; the outer summation sums these weighted by the number of nodes. When the graph is connected ($k = 1$), WASP is equivalent to the ordinary average shortest path length.

3. Meshedness Coefficient (MC)

Meshedness Coefficient measures the degree of density (tightness) between nodes in the graph, usually defined by the relationship between the number of edges and the number of cycles:

$$MC = \frac{|E| - |V| + 2}{|E|} \quad (4)$$

where $|V|$ represents the number of nodes, and $|E|$ represents the number of edges. When $|E| > |V| - 1$, cycles exist in the graph, and a larger Mesh Coefficient (MC) indicates more cycles in the graph and tighter connections between nodes.

For Metromap, each sample considers only two metrics: Graph Size (GS) and Weighted Average Shortest Path (WASP). Each indicator was first normalized and subsequently aggregated by computing their arithmetic mean. Samples are sorted by this average value and strictly divided into three levels: Hard, Medium, and Easy, with a ratio of 1:1:1. For Travelmap, the GS, WASP, and MC metrics are considered simultaneously. To ensure a balanced distribution of Map Difficulty levels in both the training and test sets, the algorithm groups every three consecutive samples after sorting. From each group, one sample is randomly selected for the test set, and the other two for the training set, thereby balancing the train/test ratio and difficulty levels.

C.2.2. QUERY DIFFICULTY CLASSIFICATION

In RP tasks, the structural characteristics of Metromap and Travelmap differ significantly: the former has many intersection points and an extremely large number of simple paths between nodes, making the calculation of the average length of all simple paths overly complex, so it is only suitable to use the Shortest Path Length Index (SPLI) for measurement. The latter has a relatively small number of simple paths, so using the Simple Path Complexity Index (SPCI) to calculate the average length of all simple paths can more objectively reflect RP difficulty.

1. Shortest Path Length Index (SPLI)

SPLI measures the shortest path length from source point s to target point t in the graph, i.e., the number of edges passed by the shortest path between points. This metric is used to evaluate the connection efficiency between nodes. For Metromap, which has many intersections and a massive number of simple paths, using only the shortest path length can effectively characterize query difficulty:

$$SPLI(s, t) = \min(L_1, L_2, \dots, L_n) \quad (5)$$

where L_i represents the length of all paths from s to t in the graph.

2. Simple Path Complexity Index (SPCI)

SPCI measures the average length of all simple paths (paths without repeating nodes) from source point s to target point t in the graph, used to characterize path complexity. A higher SPCI value indicates more selectable paths and a more complex structure. For Travelmap, it can objectively reflect the diversified connections and query difficulty between source and target points:

$$SPCI(s, t) = \frac{1}{N} \sum_{i=1}^N l(L_i) \quad (6)$$

where N is the number of all simple paths from s to t , and $l(L_i)$ is the length of path L_i .

The number of queries per image is determined by the algorithm described in Appendix B.2. Subsequently, after query generation, Query Difficulty Classification is performed for each image. In Metromap and Travelmap, queries are sorted according to their respective difficulty metrics and strictly divided into Hard, Medium, and Easy levels in equal proportions.

D. Query Template

D.1. RP Query

In this study, we design a series of RP queries based on *Metromap* and *Travelmap* to evaluate path optimization algorithms under different input modalities and constraint settings. Taking the *Map-Only* setting in *Metromap* as an example, where $\{\text{station}_1\}$ and $\{\text{station}_2\}$ denote randomly sampled origin-destination pairs described in Section 3.3.1, we formulate five types of queries with different instruction styles as follows:

1. **Direct Optimization query:** According to the Subway Map, what is the path with the fewest stations from {station_1} to {station_2}?
2. **Graph-theoretic:** According to the Subway Map, what is the shortest path from {station_1} to {station_2}?
3. **Instruction-seeking:** According to the Subway Map, how can I reach {station_2} from {station_1} via the shortest path?
4. **User-oriented Optimization:** According to the Subway Map, how can I travel from {station_1} to {station_2} with the fewest number of stations?
5. **Constraint-explicit Optimization:** According to the Subway Map, what is the shortest route in terms of station count from {station_1} to {station_2}?

All remaining queries are also constructed with these five instruction styles. For brevity, we list only the *Direct Optimization query* style below:

- **Unconstrained - Edge_tab-Only:** According to Edge Table and Vertex Table, what is the path with the fewest stations from {station_1} to {station_2}?
- **Unconstrained - Map+Edge_tab:** According to the Subway Map, Edge Table and Vertex Table, what is the path with the fewest stations from {station_1} to {station_2}?
- **Single/Multi-constraint - Map+Edge_tab+Vertex_tab:**
 1. **Time-Only:** According to the Subway Map, Edge Table and Vertex Table, what is the fastest route from {station_1} to {station_2}?
 2. **Price-Only:** According to the Subway Map, Edge Table and Vertex Table, what is the cheapest route from {station_1} to {station_2}?
 3. **Comfort Level-Only:** According to the Subway Map, Edge Table and Vertex Table, what is the smoothest ride between {station_1} and {station_2}?
 4. **Reliability-Only:** According to the Subway Map, Edge Table and Vertex Table, what is the most stable subway route from {station_1} to {station_2}?
 5. **Time+Price+Reliability:** According to the Subway Map, Edge Table and Vertex Table, what is the optimal route considering time, price, and reliability from {station_1} to {station_2}?
 6. **Time+Comfort Level+Reliability:** According to the Subway Map, Edge Table and Vertex Table, what is the fastest, most comfortable, and reliable route from {station_1} to {station_2}?
 7. **Price+Comfort Level+Reliability:** According to the Subway Map, Edge Table and Vertex Table, what is the best route optimizing price, comfort, and reliability from {station_1} to {station_2}?
 8. **Time+Price+Comfort Level+Reliability:** According to the Subway Map, Edge Table and Vertex Table, what is the optimal route considering time, price, comfort, and reliability from {station_1} to {station_2}?
- **Multi-constraint - Map+Vertex_tab:** According to the Subway Map and the Vertex Table, what is the optimal route considering time, price, comfort, and reliability from {station_1} to {station_2}?

For *Travelmap*, the term “Subway Map” is replaced with “Scenic Area Planning Map” in all queries.

D.2. QA Query

In addition to RP queries, we design a series of QA queries based on *Metromap* and *Travelmap*. The experimental setup systematically considers four input modalities: *Map-Only*, *Edge_tab-Only*, *Vertex_tab-Only*, and *Map+Vertex_tab*. For *Metromap*, the *Vertex_tab* excludes the *Line* column, enabling an explicit evaluation of multimodal joint reasoning under missing single-modality information.

Under each modality, we construct three categories of tasks: *Global Perception-based Reasoning Tasks (GP)*, *Local Perception-based Reasoning Tasks (LP)*, and *Spatial Relationship Judgment Tasks (SR)*. Each QA category is instantiated with five semantically equivalent but stylistically distinct instruction templates, including *Direct / Neutral*, *Simple & Conversational*, *Slightly Formal*, *Technical / Academic Style*, and *Concise / Dataset-Friendly*.

Taking the *Map-Only Global Perception-based Reasoning Tasks (GP)* as an example, the five instruction styles are as follows:

1. **Direct / Neutral:** How many metro lines are there in total on the Subway Map?
2. **Simple & Conversational:** How many subway lines are shown on the metro map?
3. **Slightly Formal:** What is the total number of rail lines in the Subway Map?
4. **Technical / Academic Style:** How many distinct transit lines does the metro map contain?
5. **Concise / Dataset-Friendly:** What is the total count of metro lines in the map?

All QA tasks follow the same five-style formulation. Below, we list a subset of queries using only the *Direct / Neutral* style:

1. Metromap-Map - GP: How many metro lines are there in total on the Subway Map?
2. Metromap-Map - LP: How many stations are there between {Station A} and {Station B} on the same line?
3. Metromap-Map - SR: Is {Station A} on Line X?
4. Metromap-Edge_tab - GP: What is the number of stations on the longest subway line?
5. Metromap-Edge_tab - LP: What is the Time/Price/Comfort Level value for the edge {Station A}-{Station B}?
6. Metromap-Edge_tab - SR: How many edges are there between the edge {Station A}-{Station B} and the edge {Station C}-{Station D}?
7. Metromap-Vertex_tab - GP: How many transfer stations are there in the entire table?
8. Metromap-Vertex_tab - LP: How many transfer stations are there on {Line X}?
9. Metromap-Vertex_tab - SR: Are {Station A} and {Station B} on the same line?
10. Metromap-Map+Vertex_tab - GP: What is the total stop time of the subway line with the longest stop time?
11. Metromap-Map+Vertex_tab - LP: What is the average reliability from {Station A} to {Station B} on the same line?
12. Metromap-Map+Vertex_tab - SR: Please check if there are transfer stations between {Line X} and {Line Y}. If there are, return the shortest transfer time; if not, return 0. If there is only one subway line, return 1.
13. Travelmap-Map - GP: How many tourist attractions are there in total?
14. Travelmap-Map - LP: Is scenic {Spot A} on the circular route?
15. Travelmap-Map - SR: How many scenic spots are adjacent to scenic {Spot A}?
16. Travelmap-Edge_tab - GP: How many times does the most frequently appearing scenic spot appear in the table?
17. Travelmap-Edge_tab - LP: What is the value of Time/Price for {Spot A}-{Spot B}?
18. Travelmap-Edge_tab - SR: Is the shortest distance between {Spot A} and {Spot B} less than 5?
19. Travelmap-Vertex_tab - GP: How many scenic spots in the table have a Time value less than 30?
20. Travelmap-Vertex_tab - LP: Given {Spot A}, {Spot B}, {Spot C}, and {Spot D}, what is the price of the cheapest one?
21. Travelmap-Vertex_tab - SR: Is {Spot A} located above {Spot B} in the table?
22. Travelmap-Map+Vertex_tab - GP: Is the number of scenic spots in the table the same as the actual number of scenic spots in the map?

23. Travelmap-Map+Vertex_tab - LP: Are there any locations with Time < 30 along all shortest paths from {Spot A} to {Spot B}?
24. Travelmap-Map+Vertex_tab - SR: What is the cost of the lowest-priced location adjacent to {Spot A}?

The design of this task suite ensures that the QA queries can effectively reveal the intrinsic characteristics of the dataset, thereby providing support for better training framework design in subsequent RP tasks. Moreover, the tasks span diverse modalities and reasoning challenges, offering rich instruction styles and task scenarios to comprehensively evaluate model performance.

E. Prompt Template

In this study, the prompt templates are divided into two categories: one for RP tasks and the other for QA tasks. Since the prompt construction methods for *Metromap* and *Travelmap* are identical, we take the prompts for *Metromap* as an illustrative example below.

E.1. Prompts for Generating Edge_tab and Vertex_tab

In this work, we design the *Edge_tab* and *Vertex_tab* attributes for *Metromap* and *Travelmap* based on real-world transportation networks and connectivity characteristics between metro systems and scenic areas. Specifically, the attributes in *Edge_tab* capture key operational characteristics of metro systems and scenic routes, including time, price, comfort level, and reliability, which are used to simulate the operational properties of different paths and the corresponding user experience. In contrast, the attributes in *Vertex_tab* focus on the characteristics of metro stations and scenic spots, covering dwell time, comfort level, price, reliability, and transfer time, thereby modeling the transfer complexity between stations or attractions as well as the passenger experience at each location. Through the design of these attributes, we aim to faithfully reflect the diverse factors that must be considered in RP tasks, ensuring the scientific validity and rationality of model behavior during path selection and optimization. The specific attribute designs and their underlying rationales are described below.

E.1.1. METROMAP-EDGE_TAB

Based on real-world characteristics between adjacent metro stations, we design the attributes in the *Metromap Edge_tab* as follows:

1. **Line:** This attribute indicates the metro line to which a station belongs, represented in the form of x Line, where x denotes the line number or name.
Design Rationale: This attribute is used solely to annotate the metro line associated with each segment, facilitating the distinction between different lines and clarifying the connectivity relationships between stations.
2. **Time:** This attribute simulates the travel time between Station A and Station B, with values ranging from 2.00 to 3.00 minutes, rounded to two decimal places.
Design Rationale: This range reflects typical travel durations between adjacent stations in urban metro systems.
3. **Price:** This attribute takes values ranging from 0.00 to 1.50 RMB, rounded to two decimal places.
Design Rationale: This range is intended to simulate a broad spectrum of metro fare levels, which commonly fluctuate within this interval across many cities.
4. **Comfort Level:** This attribute models passengers' perceived comfort, with values ranging from 0.00 to 1.00, rounded to two decimal places.
Design Rationale: The range from 0.00 to 1.00 represents a spectrum from extremely poor to excellent riding experiences. Considering that real-world metro comfort may be affected by factors such as carriage crowding, air quality, and noise, this range reasonably captures variations in passenger comfort perception.
5. **Reliability:** This attribute is set to 0.
Design Rationale: Since metro services would not operate if they were unreliable, all routes in this model are assumed to be reliable by default, and reliability is therefore not explicitly differentiated.

The generation prompt for *Edge_tab* in *Metromap* as implemented in the Gemini-3-Flash model is specified as follows:

```

Prompt: Metromap Edge_tab Generation

# Role
You are a table-generation agent that generates metro edge data.

# Rules
- Only output a metro Edge table. No explanations, no extra text, no code block markers.
- Generate strictly based on the provided JSON file. Do not hallucinate.
- Do not duplicate edges ('A-B' and 'B-A' count as one).
- For each Line, list all edges consecutively, then move to the next Line.
- Loop lines must form a closed loop; non-loop lines only connect adjacent stations.

# Table Format (exact)
Edge, Line, Time, Price, Comfort Level, Reliability

# Edge & Name Rules
- Edge format: 'StationA-StationB'
- If a station name contains '-', replace it with '_' and remove spaces around it
  (e.g., 'King Street -Old Town' -> 'King Street_Old Town')
- Preserve original spaces inside names (e.g., 'King Street ')
- Preserve other symbols but remove spaces around them
  (e.g., 'U Street / African' -> 'U Street/African')

# Value Constraints
- Line: 'x Line'
- Time: random, 2 decimals, 2.00-3.00
- Price: random, 2 decimals, 0.00-1.50
- Comfort Level: random, 2 decimals, 0.00-1.00
- Reliability: only 0

# Example (format only)
Edge, Line, Time, Price, Comfort Level, Reliability
Shady Grove-Rockville, Red Line, 2.20, 1.38, 0.45, 0.91
Fort Totten-Brookland, Line 1, 2.33, 1.32, 0.55, 0.77

Now start generating the Edge CSV. Wrap the CSV content strictly between '<ledge_csv_begin>' and
'<ledge_csv_end>', and ensure that the CSV syntax between these two tags is absolutely correct.

```

E.1.2. METROMAP-VERTEX_TAB

Based on real-world characteristics of metro stations, we design the attributes in the *Metromap Vertex_tab* as follows:

1. **Line:** This attribute indicates the metro line to which a station belongs, represented in the form of *x Line*, where *x* denotes the line number or name.

Design Rationale: This attribute is used to annotate the line associated with each metro station, enabling the model to distinguish stations belonging to different lines.
2. **Time:** This attribute simulates the dwell time at each metro station, with values ranging from 0.50 to 2.00 minutes, rounded to two decimal places.

Design Rationale: This attribute models the time a train stops at a station, with values determined by simulated passenger flow and station-specific characteristics.
3. **Price:** This attribute is set to 0.

Design Rationale: Since no additional cost is incurred during station dwell time, pricing is only considered during metro travel segments.
4. **Comfort Level:** This attribute models passengers' perceived comfort, with values ranging from 0.00 to 1.00, rounded to two decimal places.

MapTab: Can MLLMs Master Constrained Route Planning?

Design Rationale: The range from 0.00 to 1.00 is designed to simulate variations in boarding and alighting volumes as well as station crowding levels.

5. **Reliability:** This attribute takes values ranging from 0.50 to 1.00, rounded to two decimal places.

Design Rationale: This range simulates the probability of station disruptions and downtime caused by unexpected events (e.g., security incidents or equipment failures), reflecting reliability differences across stations.

6. **Transfer Time:** This attribute represents the time required for transfers, with values ranging from 5 to 15 minutes, specified as integers.

Design Rationale: This range reflects the time cost of transfers between stations, varying according to transfer complexity and the physical distance between metro lines.

The generation prompt for *Vertex_tab* in *Metromap* as implemented in the Gemini-3-Flash model is specified as follows:

Prompt: Metromap Vertex_tab Generation

```
# Role
You are a table-generation agent that generates metro Vertex data.

# Rules
- Strictly generate a metro Vertex table only.
- Output table content only: no explanations, no extra text, no notes, no comments, no code block markers.
- Generate strictly based on the given JSON file. Do not hallucinate.
- Remove duplicate vertices: if a vertex appears multiple times, keep only the first occurrence.
- For each Line, list all vertices in order, then move on to the next Line.

# Table Format (exact)
Vertex, Line, Time, Price, Comfort Level, Reliability, Transfer Time

# Vertex Rules
- Vertex format: 'StationName' (e.g., 'Shady Grove', 'Rockville', 'Twinbrook')

# Special Character Handling Rules
1. Replace '-' with '_' and remove spaces if the station name originally contains '-'
   (e.g., 'King Street -Old Town' -> 'King Street_Old Town')
2. Preserve original spaces inside names (e.g., 'King Street ')
3. Preserve other symbols but remove spaces around them
   (e.g., 'U Street / African' -> 'U Street/African')

# Column Value Constraints
- Line: 'x Line'
- Time: random, 2 decimals, 0.50-2.00
- Price: only 0
- Comfort Level: random, 2 decimals, 0.00-1.00
- Reliability: random, 2 decimals, 0.50-1.00
- Transfer Time: random, integers, 5-15

# Example (format only)
Vertex, Line, Time, Price, Comfort Level, Reliability, Transfer Time
Fort Totten, Line 1|Line 2, 1.38, 0, 0.38, 0.75, 6
Chow, Red Line|Green Line, 1.55, 0, 0.92, 0.66, 9

Now start generating the Vertex CSV. Wrap the CSV content strictly between '<|vertex_csv_begin|>' and '<|vertex_csv_end|>', and ensure that the CSV syntax between these two tags is absolutely correct.
```

E.1.3. TRAVELMAP-EDGE_TAB

Based on real-world transportation networks and road connectivity characteristics between tourist attractions, we design the attributes in the *Travelmap Edge_tab* as follows:

1. **Time:** This attribute simulates the commuting time from one attraction to another. If the map explicitly provides a time annotation, that value is directly used. If only distance information is available and the distance exceeds 1 km, the time is computed assuming a speed of 60 km/h. If the distance is less than 1 km, a speed of 4 m/s is assumed and the resulting time is converted into minutes. Any computed time shorter than 1 minute is rounded up to 1 minute. If neither time nor distance information is provided, a random integer between 10 and 60 minutes is generated.
Design Rationale: Commuting time is inferred from the time or distance annotations provided on the map, or otherwise simulated using reasonable assumptions based on common transportation knowledge.
2. **Price:** This attribute is a randomly generated integer ranging from 10 to 80, with smaller values occurring more frequently.
Design Rationale: This attribute simulates commuting costs, reflecting price variations across different routes or transportation modes. The biased random generation toward lower prices captures realistic cost distribution patterns observed in daily travel.
3. **Comfort Level:** This attribute models passengers' perceived comfort using a travel-review-style rating scheme (e.g., from tourism applications such as Ctrip or Dianping). A single-decimal value is randomly generated within the range of 1.0 to 5.0, with ratings ≥ 3.0 accounting for the majority.
Design Rationale: This attribute simulates comfort experiences across different routes or transportation modes, where higher comfort scores are typically associated with better vehicles, routes, or environmental conditions.
4. **Reliability:** This attribute is defined as $a/365$, where a is an integer ranging from 1 to 365, with values greater than 180 occurring more frequently. The final value is reported with six decimal places. **Design Rationale:** This attribute simulates route reliability by accounting for potential disruptions such as road construction, security controls, or closures of high-risk areas. Here, a represents the number of days a route is effectively accessible within a year; larger values indicate higher reliability, reflecting lower frequencies of closures or access restrictions due to special events.

The generation prompt for *Edge_tab* in *Travelmap*, as implemented in the Gemini-3-Flash model, is specified as follows:

Prompt: Travelmap Edge_tab Generation

```
# Role
You are a **table-generation agent** that generates **tourist attraction (scenic area) edge data** based on a map.

# Rules
- **Strictly generate an Edge table only.**
- **Output table content only**: no explanations, no extra text, no notes, no comments, no code block markers.
- **Generate strictly based on the given scenic map image. Do not hallucinate.**
- **Only list valid Edges**: an Edge exists only if two attractions are directly connected on the map.
- **Do not duplicate Edges**: 'A-B' and 'B-A' are the same and must appear only once.
- List Edges **top to bottom first, then left to right**, following the spatial order of the map.

# Table Format (exact)
Edge, Time, Price, Comfort Level, Reliability

# Edge Rules
- Edge format: 'AttractionA - AttractionB'
(e.g., 'MUJI YOUSELF-Rockefeller Center', 'Rockefeller Center-Nintendo')
- Preserve original spaces inside names (e.g., 'Rockefeller Center')
- Preserve other symbols but remove spaces around them
(e.g., 'St. Patrick's Cathedral' -> 'St. Patrick's Cathedral')

# Value Constraints
- **Time**: minutes only; if shown on the map convert directly ('24 minutes' -> '24', '2 hours' -> '120'); if distance is provided and  $> 1$  km, compute time using  $60$  km/h; if distance is  $< 1$  km, compute time using  $4$  m/s and convert to minutes; any result  $< 1$  minute is rounded up to 1 minute; if neither time nor distance is shown, generate a random integer  $10-60$ 
- **Price**: random integer  $10-80$ , with smaller values appearing more frequently
- **Comfort Level**: travel review style rating, random one-decimal  $1.0-5.0$ , values  $\geq 3.0$  should be the
```

MapTab: Can MLLMs Master Constrained Route Planning?

```
majority
- Reliability: defined as 'a/365', where 'a' is an integer 1-365, values with a > 180 should be the
  majority, output as a decimal with six digits

# Example (format only)
Edge, Time, Price, Comfort Level, Reliability
MUJI YOUSELF-Rockefeller Center, 24, 20, 2.3, 0.928767
Rockefeller Center-Nintendo, 18, 15, 2.4, 0.805479

Now start generating the Vertex CSV. Wrap the CSV content strictly between '<| vertex_csv_begin |>' and
'<| vertex_csv_end |>', and ensure that the CSV syntax between these two tags is absolutely correct.
```

E.1.4. TRAVELMAP-VERTEX_TAB

Based on real-world characteristics of tourist attractions and transportation facilities, we design the attributes in the *Travelmap Vertex_tab* as follows:

- Time**: This attribute is generated as a random integer in the range of 30-180 minutes. For locations such as airports and railway stations, the time is directly set to 0.
Design Rationale: This attribute is intended to simulate the duration of stay at each attraction. Locations such as airports and stations typically do not involve sightseeing activities, and thus their time values are set to 0.
- Price**: This attribute is a random integer ranging from 10 to 200 and constrained to be a multiple of 5. For locations such as airports and railway stations, the price is randomly set to 100, 200, or 300.
Design Rationale: This attribute simulates entrance fees for attractions and service costs at transportation hubs. In RP tasks, transportation station costs are counted only at the final destination, while prices at intermediate stations are set to 0, reflecting the cost structures of different attractions and transportation facilities.
- Comfort Level**: This attribute models perceived comfort using a travel-review-style rating scheme. A single-decimal value is randomly generated within the range of 1.0-5.0, with ratings ≥ 3.0 accounting for the majority.
Design Rationale: This design simulates tourists' comfort experiences when visiting attractions or using services at transportation hubs.
- Reliability**: This attribute is defined as $a/365$, where a is an integer ranging from 60 to 365, with values greater than 180 occurring more frequently. The final value is reported with six decimal places.
Design Rationale: This attribute simulates the reliability of different attractions or transportation facilities, reflecting whether attractions are open and whether transportation hubs experience service suspensions or closures. Here, a denotes the number of days per year during which the location is operational; larger values indicate higher reliability.

The generation prompt for *Vertex_tab* in *Travelmap*, as implemented in the Gemini-3-Flash model, is specified as follows:

Prompt: Travelmap Vertex_tab Generation

```
# Role
You are a table-generation agent that generates tourist attraction (scenic area) vertex data based on a map.

# Rules
- Strictly generate a Vertex table only.
- Output table content only: no explanations, no extra text, no notes, no comments, no code block markers.
- Generate strictly based on the given scenic map image. Do not hallucinate.
- Only list valid Vertices: a Vertex must appear as a scenic attraction on the map.
- Do not duplicate Vertices: if the same attraction appears multiple times, list it only once.
- List Vertices top to bottom first, then left to right, following the spatial order of the map.

# Table Format (exact)
Vertex, Time, Price, Comfort Level, Reliability
```

```

# Vertex Rules
- Vertex format: 'AttractionName'
(e.g., 'MUJI YOUSELF', 'Rockefeller Center', 'Nintendo')
- Preserve original spaces inside names.
(e.g., 'Rockefeller Center')
- Preserve other symbols but remove spaces around them
(e.g., 'St. Patrick's Cathedral' -> 'St. Patrick's Cathedral')

# Value Constraints
- **Time**: random integer **30-180**, set to **0** for places like airports, train stations, etc.
- **Price**: random integer multiple of 5 in **10-200**
- **Comfort Level**: travel review style rating, random value in **1.0-5.0** with one decimal place, values >= 3.0 should be the majority
- **Reliability**: defined as 'a/365', where 'a' is an integer 60-365, values with a > 180 should be the majority, output as a decimal with six digits

# Example (format only)
Vertex, Time, Price, Comfort Level, Reliability
MUJI YOUSELF, 41, 45, 4.9, 0.975342
Rockefeller Center, 43, 100, 4.6, 0.745205
Nintendo, 21, 55, 4.3, 0.380822

Now start generating the Vertex CSV. Wrap the CSV content strictly between '<|vertex_csv_begin|>' and '<|vertex_csv_end|>', and ensure that the CSV syntax between these two tags is absolutely correct.
    
```

E.2. Prompts for RP Queries

For RP tasks, the prompts in the Metromap dataset are divided into a total of 12 categories. Among them, three categories correspond to unconstrained prompts under different input modalities, namely Map-only, Edge_tab-only, and Map+Edge_tab. The remaining nine categories involve prompts with single or multiple constraints.

Furthermore, in constrained Metromap scenarios, in order to enable a comprehensive consideration of different evaluation dimensions, normalization or transformation operations are applied to the indicators Time, Price, Comfort Level, Reliability, and Transfer Time. The specific preprocessing rules are as follows:

1. **Time**: The original value range $[0, 3]$ is linearly scaled to $[0, 1]$.
2. **Price**: The original value range $[0, 1.5]$ is linearly scaled to $[0, 1]$.
3. **Transfer Time**: The original value range $[5, 15]$ is scaled according to the same benchmark ratio as $[0, 3]$, so as to ensure that transfer behaviors are assigned a significant penalty weight.
4. **Comfort Level and Reliability**: Comfort and reliability (originally in the range $[0, 1]$) are subjected to an inverse transformation (i.e., $1 - x$) when jointly considered with other factors, and zero values are removed.

Similarly, for constrained Travelmap datasets, the four indicators, Time, Price, Comfort Level, and Reliability, also require corresponding scaling or inversion operations. The specific rules are as follows:

1. **Time**: The original value range $[0, 180]$ is linearly scaled to $[0, 1]$. If the range is larger, scaling is still performed based on the $[0, 180]$ interval.
2. **Price**: The original value range $[0, 200]$ is linearly scaled to $[0, 1]$. If the range is larger, scaling is still performed based on the $[0, 200]$ interval.
3. **Comfort Level**: The original value range $[0, 5]$ is linearly scaled to $[0, 1]$.
4. **Comfort Level and Reliability**: Comfort and reliability (in the range $[0, 1]$) are subjected to an inverse transformation (i.e., $1 - x$) when jointly considered with other factors, and zero values are removed.

MapTab: Can MLLMs Master Constrained Route Planning?

In addition, to construct *Vertex2_tab*, we integrate part of the information from *Edge_tab* into *Vertex_tab*. The merging strategy is as follows: in Metromap, the *Price* column of *Vertex2_tab* is computed as the mean price of all edges associated with the corresponding node in *Edge_tab*, while the remaining attributes remain identical to those in the original *Vertex_tab*. In Travelmap, all attribute values from the original *Vertex_tab* are directly retained without any integration.

In the following, we only elaborate on the prompts adopted by the five experimental configurations listed in Table 4.2.1.

Prompt: Unconstrained Query (Map-Only)

Role

You are a Subway Pathfinding Algorithm. You strictly analyze the provided metro map, and compute the shortest -stop route .

Input Task

{ question }

Objective

Return only one final route - the one with the absolute minimum number of stops.

A station cannot appear more than once in the route. Cannot reselect the path that has already been taken!

If multiple routes have the same number of stops, randomly select one of them.

Output Format Constraints

- **Separator**: Use hyphens '-' strictly, with **no spaces** around the hyphens.

- **Transfer Marking**: If and only if a line transfer occurs at a station, append '(transfer)' immediately after its name.

- **Content**: Output only the final route string. No markdown, no explanation, no filler .

Few-Shot Output Examples

Notice that this is only the output format example. In real question we will give you an image as map for you to figure out the shortest path.

Example 1

User: Path from Summerhill to Woodbine

Assistant : Summerhill-Rosedale-Bloor_Yonge(transfer)-Sherbourne-Castle
Frank-Broadview-Chester-Pape-Donlands-Greenwood-Coxwell-Woodbine

Example 2

User: Path from Viktoria_Luise_Platz to Jakob_Kaiser_Platz

Assistant : Viktoria_Luise_Platz - Nollendorfplatz (transfer)- Wittenbergplatz (transfer)-Augsburger
StraSse-SpichernstraSse(transfer)- Berliner StraSse(transfer)-BlissestraSse-Konstanzer
StraSse-Adenauerplatz-Wilmersdorfer
StraSse-Richard_Wagner_Platz-Mierendorffplatz- Jungfernheide - Jakob_Kaiser_Platz

Prompt: Unconstrained Query (Edge_tab-Only)

Role

You are a Subway Pathfinding Algorithm. You strictly analyze the tabular (Edge Table), and compute the shortest -stop route .

Input Task

{ question }

Objective

Return only one final route - the one with the absolute minimum number of stops.

A station cannot appear more than once in the route. Cannot reselect the path that has already been taken!

If multiple routes have the same number of stops, randomly select one of them.

Output Format Constraints

- **Separator**: Use hyphens '-' strictly, with **no spaces** around the hyphens.

- **Transfer Marking**: If and only if a line transfer occurs at a station, append '(transfer)' immediately after its name.

MapTab: Can MLLMs Master Constrained Route Planning?

- **Content**: Output only the final route string . No markdown, no explanation, no filler .

Few-Shot Output Examples

Notice that this is only the output format example. In real question we will give you a tabular (Edge Table) for you to figure out the shortest path.

Example 1

User: Path from Summerhill to Woodbine

Assistant : Summerhill-Rosedale-Bloor_Yonge(transfer)-Sherbourne-Castle
Frank-Broadview-Chester-Pape-Donlands-Greenwood-Coxwell-Woodbine

Example 2

User: Path from Viktoria_Luise_Platz to Jakob_Kaiser_Platz

Assistant : Viktoria_Luise_Platz - Nollendorfplatz (transfer)- Wittenbergplatz (transfer)-Augsburger
StraSse-SpichernstraSse(transfer)- Berliner StraSse(transfer)-BlissestraSse-Konstanzer
StraSse-Adenauerplatz-Wilmersdorfer
StraSse-Richard_Wagner_Platz-Mierendorffplatz- Jungfernheide - Jakob_Kaiser_Platz

Prompt: Unconstrained Query (Map+Edge_tab)

Role

You are a Subway Pathfinding Algorithm. You strictly analyze the provided metro map, a tabular (Edge Table), and compute the shortest -stop route .

Input Task

{ question }

Objective

Return only one final route - the one with the absolute minimum number of stops.

A station cannot appear more than once in the route . Cannot reselect the path that has already been taken!

If multiple routes have the same number of stops , randomly select one of them.

Output Format Constraints

- **Separator**: Use hyphens '-' strictly , with **no spaces** around the hyphens.

- **Transfer Marking**: If and only if a line transfer occurs at a station , append '(transfer)' immediately after its name.

- **Content**: Output only the final route string . No markdown, no explanation, no filler .

Few-Shot Output Examples

Notice that this is only the output format example. In real question we will give you an image as map and a tabular (Edge Table) for you to figure out the shortest path.

Example 1

User: Path from Summerhill to Woodbine

Assistant : Summerhill-Rosedale-Bloor_Yonge(transfer)-Sherbourne-Castle
Frank-Broadview-Chester-Pape-Donlands-Greenwood-Coxwell-Woodbine

Example 2

User: Path from Viktoria_Luise_Platz to Jakob_Kaiser_Platz

Assistant : Viktoria_Luise_Platz - Nollendorfplatz (transfer)- Wittenbergplatz (transfer)-Augsburger
StraSse-SpichernstraSse(transfer)- Berliner StraSse(transfer)-BlissestraSse-Konstanzer
StraSse-Adenauerplatz-Wilmersdorfer
StraSse-Richard_Wagner_Platz-Mierendorffplatz- Jungfernheide - Jakob_Kaiser_Platz

Prompt: Multi-Constrained Query (Map+Edge_tab+Vertex_tab)

Role

You are a Subway Pathfinding Algorithm. You strictly analyze the provided metro map, two tabulars (an Edge Table and a Vertex Table), and compute the best overall route based on weighted Time, Price, Comfort Level, and Reliability .

MapTab: Can MLLMs Master Constrained Route Planning?

Input Task

{question}

Objective

The route should be planned for a family trip . Time, Price, Comfort Level, and Reliability must be considered together according to the weight proportions {w1}, {w2}, {w3}, {w4}. Return only one final route - the one you believe is the best overall choice based on these weighted factors .

A station cannot appear more than once in the route . Cannot reselect the path that has already been taken!

Note: Total Time includes Commuting Time of each edge, Standing Time of each vertex and Transfer Time from stations . Transfer Time is only added when a line transfer occurs; stations passed without transferring do not contribute Transfer Time.

Input Data Description

The input consists of:

1. One metro map image
2. An **Edge Table**: each edge contains 'Time', 'Price', 'Comfort Level', and 'Reliability' attributes representing travel time, monetary cost, ride comfort, and route reliability
3. A **Vertex Table**: each station contains 'Time', 'Price', 'Comfort Level', 'Reliability', and 'Transfer Time'
 - 'Time': time spent at the station
 - 'Price': monetary cost at the station
 - 'Comfort Level': comfort at the station
 - 'Reliability': reliability at the station
 - 'Transfer Time': time penalty added only when a line transfer occurs at that station

Attributes Scaling Rules

1. All 'Time' values, originally within 0-3, must be proportionally scaled into 0-1
2. All 'Price' values, originally within 0-1.5, must be proportionally scaled into 0-1
3. 'Transfer Time' values, originally 5-15, must be scaled using the same 0-3 proportion, ensuring transferring carries a significant penalty
4. All 'Comfort Level' and 'Reliability' values, ranging from 0-1, must be converted into one minus their values for scoring, excluding zero values

Pathfinding Requirements

1. The metro network must be treated as a heterogeneous weighted graph where edges receive weights from the Edge Table and stations receive weights from the Vertex Table
2. Total Time includes Commuting Time of each edge, Standing Time of each vertex, and Transfer Time from stations, applied only when a line transfer occurs
3. All attribute values of the destination station are excluded from evaluation; starting station attributes are fully included
4. When weight proportions {w1}, {w2}, {w3}, {w4} are provided, the final route score is computed by combining normalized Time, normalized Price, converted Comfort Level, and converted Reliability according to these proportions
5. The system must output only the single route with the best overall score

Output Format Constraints

- **Separator**: Use hyphens '-' strictly, with no spaces around the hyphens
- **Transfer Marking**: If a line transfer occurs at a station, append '(transfer)' immediately after its name
- **Content**: Output only the final route string. No markdown, no explanation, no filler

Few-Shot Output Examples

Notice that these are only formatting examples. Actual routes depend on the provided map and tables .

Example 1

User: Path from Summerhill to Woodbine

Assistant : Summerhill-Rosedale-Bloor_Yonge(transfer)-Sherbourne-Castle
Frank-Broadview-Chester-Pape-Donlands-Greenwood-Coxwell-Woodbine

Example 2

User: Path from Viktoria_Luise_Platz to Jakob_Kaiser_Platz

Assistant : Viktoria_Luise_Platz - Nollendorfplatz (transfer) - Wittenbergplatz (transfer) - Augsburg
StraSse-SpichernstraSse(transfer) - Berliner StraSse(transfer) - BlissestraSse-Konstanzer
StraSse-Adenauerplatz-Wilmersdorfer

StraSse-Richard_Wagner_Platz-Mierendorffplatz- Jungfernheide - Jakob_Kaiser_Platz

Prompt: Multi-Constrained Query (Map+Vertex2_tab)

Role

You are a Subway Pathfinding Algorithm. You strictly analyze the provided metro map and the Vertex Table, and compute the best overall route based on weighted Time, Price, Comfort Level, and Reliability .

Input Task

{ question }

Objective

The route should be planned for a family trip . Time, Price, Comfort Level, and Reliability must be considered together according to the weight proportions {w1}, {w2}, {w3}, {w4}. Return only one final route - the one you believe is the best overall choice based on these weighted factors .

A station cannot appear more than once in the route . Cannot reselect the path that has already been taken!

Note: Total Time includes both Standing Time of each vertex and Transfer Time from stations . Transfer Time is only added when a line transfer occurs; stations passed without transferring do not contribute Transfer Time.

Input Data Description

The input consists of:

1. One metro map image
2. A **Vertex Table**: each station contains 'Time', 'Price', 'Comfort Level', 'Reliability', and 'Transfer Time'
 - 'Time': time spent at the station
 - 'Price': monetary cost at the station
 - 'Comfort Level': comfort at the station
 - 'Reliability': reliability at the station
 - 'Transfer Time': time penalty added only when a line transfer occurs at that station

Attributes Scaling Rules

1. All 'Time' values, originally within 0-3, must be proportionally scaled into 0-1
2. All 'Price' values, originally within 0-1.5, must be proportionally scaled into 0-1
3. 'Transfer Time' values, originally 5-15, must be scaled using the same 0-3 proportion, ensuring transferring carries a significant penalty
4. All 'Comfort Level' and 'Reliability' values, ranging from 0-1, must be converted into one minus their values for scoring, excluding zero values

Pathfinding Requirements

1. The metro network must be treated as a heterogeneous weighted graph where stations receive weights from the Vertex Table
2. Total Time includes both Standing Time of each vertex and Transfer Time from stations, applied only when a line transfer occurs
3. All attribute values of the destination station are excluded from evaluation; starting station attributes are fully included
4. When weight proportions {w1}, {w2}, {w3}, {w4} are provided, the final route score is computed by combining normalized Time, normalized Price, converted Comfort Level, and converted Reliability according to these proportions
5. The system must output only the single route with the best overall score

Output Format Constraints

- **Separator**: Use hyphens '-' strictly, with no spaces around the hyphens
- **Transfer Marking**: If a line transfer occurs at a station, append '(transfer)' immediately after its name
- **Content**: Output only the final route string . No markdown, no explanation, no filler

Few-Shot Output Examples

Notice that these are only formatting examples. Actual routes depend on the provided map and tables .

Example 1

User: Path from Summerhill to Woodbine

Assistant : Summerhill-Rosedale-Bloor_Yonge(transfer)-Sherbourne-Castle
Frank-Broadview-Chester-Pape-Donlands-Greenwood-Coxwell-Woodbine

```
## Example 2
User: Path from Viktoria_Luise_Platz to Jakob_Kaiser_Platz
Assistant : Viktoria_Luise_Platz - Nollendorfplatz ( transfer )- Wittenbergplatz ( transfer )-Augsburger
StraSse-SpichernstraSse(transfer)- Berliner StraSse(transfer)-BlissestraSse-Konstanzer
StraSse-Adenauerplatz-Wilmersdorfer
StraSse-Richard_Wagner_Platz-Mierendorffplatz- Jungfernheide - Jakob_Kaiser_Platz
```

E.3. Prompts for QA Queries

For the QA tasks, a total of 24 questions are designed across the Metromap and Travelmap scenarios. In Metromap, four input modalities: *Map-Only*, *Edge_Tab-Only*, *Vertex_Tab-Only*, and *Map + Vertex Tab* are considered, covering three categories of problems: Global Perception-based Reasoning tasks (GP), Local Perception-based Reasoning tasks (LP), and Spatial Relationship Judgment tasks (SR). This paper reports only the prompts corresponding to the *Map + Vertex_Tab* input setting.

Prompt: Map+Vertex Tab-GP

```
# Role
You are an algorithm that determines the total stop time of the subway line with the longest total stop time.
You must strictly analyze the provided map image and the Vertex Table and compute which subway line has the
maximum total stop time and what that total time is.

# Input Task
{ question }

# Requirements
## For the map
- Do NOT use any prior knowledge, memory, or real-world assumptions.
  You must rely only on what is visually present in the given map.
- The Subway Map provides all station information for each line, which must be used to sum the stop times of
  each line .
- Branches are counted as separate lines and must NOT be merged into the main line .
- If a line changes its name, and the new name is completely different from the previous one,
  then each distinct name is treated as a separate line.
  (This is different from branches.)
- If the same line is visually disconnected, it is still considered one single line.
- If a line splits into multiple paths, all stations on all split paths are included in the total stop time
  of that line .
- Only lines whose stations have valid 'time' values should be counted.
  Lines with no 'time' values at all must be excluded entirely.
- Lines without a name should NOT be counted.
- Lines without stations should NOT be counted.
- Be careful not to misidentify rivers, roads, or other non-transit visual elements as subway lines .

## For the Vertex Table
- Each station's stop time must be obtained only from the 'time' column of the Vertex Table.

# Output Format Constraints
- Return one numeric value only, rounded to two decimal places.
- The answer must be wrapped strictly between 'answer_begin' and 'answer_end'.
- Output only the final answer delimited by 'answer_begin' and 'answer_end'. No markdown, no explanation,
  no extra text .

# Few-Shot Output Examples
> Note: These are only format examples.
> In the real task, you will be given an image map and a Vertex Table.

## Example 1
User: What is the total stop time of the subway line with the longest stop time?
Assistant : <answer_begin>30.55<answer_end>
```

MapTab: Can MLLMs Master Constrained Route Planning?

Example 2

User: How long is the total stop time for the subway line with the longest stops?

Assistant : <answer_begin>77.89<answer_end>

Prompt: Map+Vertex Tab-LP

Role

You are an algorithm that determines **the average reliability from station A to station B along the same subway line**.

You must strictly analyze the provided **map image and the Vertex Table** and compute **the average reliability of all stations between A and B on that line**.

Input Task

{question}

Requirements

For the map

- **Do NOT use any prior knowledge, memory, or real-world assumptions.** You must rely **only** on what is visually present in the given map.
- Collect **all stations on that line between station A and station B**, **including station A and station B themselves**.
- Be careful **not to misidentify rivers, roads, or other non-transit visual elements** as subway lines.

For the Vertex Table

- Each station's **reliability value** must be obtained **only from the 'reliability' column of the Vertex Table**.

Output Format Constraints

- Return **one numeric value only**, **rounded to two decimal places**.
- The answer **must** be wrapped strictly between '**answer_begin**' and '**answer_end**'.
- Output **only** the final answer delimited by '**answer_begin**' and '**answer_end**'. No markdown, no explanation, no extra text.

Few-Shot Output Examples

> Note: These are **only format examples**.

> In the real task, you will be given an **image map and a Vertex Table**.

Example 1

User: What is the average reliability from station A to station B on the same line?

Assistant : <answer_begin>30.55<answer_end>

Example 2

User: Could you provide the average reliability for the route between station A and station B along the same line?

Assistant : <answer_begin>77.89<answer_end>

Prompt: Map+Vertex Tab-SR

Role

You are an algorithm that determines **whether there are transfer stations between Line X and Line Y**.

If transfer stations exist, return **the shortest transfer time**; if not, return **0**.

You must strictly analyze the provided **map image and the Vertex Table** to make this determination.

Input Task

{question}

Requirements

For the map

- **Do NOT use any prior knowledge, memory, or real-world assumptions.** You must rely **only** on what is visually present in the given map.
- To determine whether **Line X and Line Y intersect**, inspect the map to see **whether they share any common station(s)**.

MapTab: Can MLLMs Master Constrained Route Planning?

```
- Identify all intersection ( transfer ) stations between Line X and Line Y shown on the map.
- If no intersection stations exist return 0 directly .
- Be careful not to misidentify rivers , roads , spots from other lines , or any unrelated visual elements as
  subway lines or stations .

## For the Vertex Table
- For each identified transfer station , obtain its transfer time from the 'transfer time' column of the
  Vertex Table .
- Compare the transfer times of all transfer stations and select the minimum value.

# Output Format Constraints
- Return a positive integer or 0 only.
  - A positive integer means the minimum transfer time among all transfer stations between Line X and Line
    Y.
  - '0' means Line X and Line Y do not intersect .
- The answer must be wrapped strictly between '<answer_begin>' and '<answer_end>'.
- Output only the final answer delimited by '<answer_begin>' and '<answer_end>'. No markdown, no explanation,
  no extra text .

# Few-Shot Output Examples
> Note: These are only format examples.
> In the real task , you will be given an image map and a Vertex Table.

## Example 1
User: Please check if there are transfer stations between Line X and Line Y. If there are , return the shortest
transfer time; if not, return 0.
Assistant : <answer_begin>0<answer_end>

## Example 2
User: Can you see if there are any transfer stations between Line X and Line Y? If so, let me know the shortest
transfer time. If not, just return 0.
Assistant : <answer_begin>6<answer_end>
```

F. More Experiments

F.1. Experimental Settings

F.1.1. MODEL SELECTION CRITERIA

Model selection is guided by evaluation requirements centered on the RP task, and two filtering criteria are applied accordingly:

1. Models that cannot meet long-context requirements are excluded (e.g., DeepSeek-VL2 (Wu et al., 2024)), as the input length of some samples exceeds 32k tokens.
2. Models that support long-context inputs but tend to exhibit reasoning loops or excessive deliberation in complex RP tasks, resulting in unstable or poorly structured outputs, are also excluded, such as llava-v1.6-mistral-hf (7B) (Liu et al., 2023), Ovis2.5 (9B) (Lu et al., 2025b), and Glyph (10B) (Cheng et al., 2025).

F.1.2. MODEL PARAMETER SETTINGS

Open-source models are primarily evaluated using the vLLM inference framework on a cluster equipped with four NVIDIA A100 GPUs. To ensure reproducibility, all experiments uniformly set `temperature` to 0.0, `maximum_generation_length` to 2,048 tokens, and extend `max_model_len` to the maximum supported by each model. Some open-source models are accessed via third-party APIs, with other parameters kept at official default settings; closed-source models are evaluated through their official APIs, following the default configurations specified in the corresponding technical documentation. For models equipped with a Thinking mechanism, the `thinking_budget` is uniformly set to 4,096 tokens.

MapTab: Can MLLMs Master Constrained Route Planning?

Table 4. Performance of QA tasks across multiple MLLMs in the Metromap and Travelmap scenarios. Regarding input modalities, M, E, and V denote Map, Edge_tab, and Vertex_tab, respectively. In the Metromap scenario, the Vertex_tab paired with the Map input has the Line column removed to prevent excessive table information from affecting the evaluation of map-table coordination. Task types are categorized into three classes: Global Perception-based Reasoning Tasks (GP), Local Perception-based Reasoning Tasks (LP), and Spatial Relationship Judgment Tasks (SR). Bold values in the table indicate the best performance among open-source and closed-source models, respectively.

Model	Type	Map (M)			Edge (E)			Vertex (V)			Map+Vertex (M+V)		
		GP	LP	SR	GP	LP	SR	GP	LP	SR	GP	LP	SR
Scenario: MetroMap													
<i>Open-source Models</i>													
Qwen3-VL-8B-Instruct	Instruct	55.00	17.50	73.12	22.50	100.0	7.50	57.50	51.88	86.88	0.63	22.50	38.75
Qwen3-VL-8B-Thinking	Thinking	53.12	28.12	51.25	56.87	99.38	56.87	79.37	77.50	98.12	7.50	9.38	35.63
Qwen3-VL-2B-Instruct	Instruct	8.13	5.00	63.12	3.75	87.50	3.12	26.25	11.25	64.38	0.00	8.13	26.87
Qwen2.5-VL-7B-Instruct	Instruct	48.75	15.62	66.25	15.62	100.0	10.00	44.37	60.62	87.50	1.25	25.62	33.12
Phi-3.5-Vision-Instruct-4B	Instruct	58.13	18.75	78.12	22.50	100.0	21.88	53.75	66.87	98.12	0.63	21.25	40.00
Phi-4-Multimodal-Instruct-6B	Instruct	60.62	40.62	80.00	41.25	93.13	42.50	58.75	92.50	99.38	5.63	35.63	49.38
InternVL3-8B-Instruct	Instruct	35.00	20.62	65.00	7.50	83.13	3.12	33.75	10.00	70.63	0.00	12.50	28.12
Qwen3-VL-30B-A3B-Instruct	Instruct	20.62	16.25	60.62	0.63	68.75	1.25	0.00	1.25	68.75	0.00	11.25	18.12
Qwen3-VL-32B-Instruct	Instruct	5.00	0.00	38.12	10.62	78.12	3.12	16.25	4.37	73.12	0.00	7.50	23.75
Qwen3-VL-32B-Thinking	Thinking	26.87	19.38	50.00	5.00	99.38	5.00	21.25	25.00	85.62	0.00	6.88	60.62
<i>Closed-source Models</i>													
GPT4-o	Instruct	62.50	13.75	78.75	31.87	100.0	28.12	55.63	78.12	100.0	3.75	29.38	45.00
GPT4.1	Instruct	61.88	26.87	76.25	50.62	99.38	38.12	64.38	83.75	100.0	3.12	25.62	49.38
Gemini-3-Flash-Preview	Instruct	59.38	82.50	93.13	91.25	98.12	75.62	88.75	94.37	100.0	48.13	80.00	94.37
Doubao-Seed-1-6-251015-w/o_Thinking	No-Thinking	55.63	20.62	76.25	41.88	100.0	59.38	58.13	86.25	99.38	3.75	49.38	50.62
Doubao-Seed-1-6-251015-Thinking	Thinking	54.37	40.62	77.50	72.50	100.0	69.37	96.25	98.75	100.0	27.50	50.00	53.12
Qwen-VL-Plus-w/o_Thinking	No-Thinking	60.00	21.88	78.75	40.62	100.0	40.00	64.38	77.50	97.50	1.25	25.62	40.62
Qwen-VL-Plus-Thinking	Thinking	57.50	45.00	81.87	68.75	100.0	71.25	90.62	95.63	100.0	13.75	46.25	55.63
Scenario: TravelMap													
<i>Open-source Models</i>													
Qwen3-VL-8B-Instruct	Instruct	7.14	60.12	52.98	17.86	99.40	45.24	38.69	50.60	61.31	75.60	70.24	14.29
Qwen3-VL-8B-Thinking	Thinking	39.29	70.83	52.38	87.50	100.0	39.88	100.0	100.0	100.0	63.10	69.05	13.69
Qwen3-VL-2B-Instruct	Instruct	12.50	58.93	9.52	6.00	94.64	64.88	1.19	46.43	38.10	64.29	67.86	4.17
Qwen2.5-VL-7B-Instruct	Instruct	4.76	65.48	54.17	38.10	99.40	47.62	17.26	87.50	79.76	33.93	68.45	16.07
Phi-3.5-Vision-Instruct-4B	Instruct	13.10	48.21	59.52	39.88	99.40	41.07	50.00	75.60	77.38	72.02	74.40	10.71
Phi-4-Multimodal-Instruct-6B	Instruct	44.05	70.24	58.93	78.57	98.81	33.93	96.43	98.21	100.0	73.21	69.05	17.86
InternVL3-8B-Instruct	Instruct	12.50	59.52	35.71	8.93	97.62	49.40	10.71	50.00	51.79	70.83	67.86	4.76
Qwen3-VL-30B-A3B-Instruct	Instruct	5.95	50.60	6.55	7.74	86.31	52.38	8.93	44.64	45.24	54.76	35.12	2.98
Qwen3-VL-32B-Instruct	Instruct	0.00	42.26	14.88	11.31	63.69	38.31	18.45	45.83	47.62	27.98	63.69	5.95
Qwen3-VL-32B-Thinking	Thinking	8.33	60.12	23.21	1.19	97.02	44.64	10.12	38.69	56.55	69.05	66.67	5.95
<i>Closed-source Models</i>													
GPT4-o	Instruct	11.31	63.69	49.40	47.02	100.0	36.31	53.57	99.40	67.26	71.43	73.21	11.31
GPT4.1	Instruct	3.57	69.64	55.95	47.02	100.0	42.86	66.07	100.0	69.64	73.21	77.38	17.86
Gemini-3-Flash-Preview	Instruct	45.83	85.12	77.98	97.62	99.40	86.31	100.0	99.40	100.0	85.71	81.55	26.19
Doubao-Seed-1-6-251015-w/o_Thinking	No-Thinking	22.62	58.93	50.00	63.10	98.81	51.79	54.76	100.0	98.81	66.07	76.79	25.60
Doubao-Seed-1-6-251015-Thinking	Thinking	24.40	71.43	55.95	95.83	84.52	71.43	97.62	100.0	100.0	78.57	72.02	22.02
Qwen-VL-Plus-w/o_Thinking	No-Thinking	19.64	72.02	52.98	48.81	100.0	35.71	57.74	98.81	82.74	54.17	70.24	19.64
Qwen-VL-Plus-Thinking	Thinking	24.40	67.86	62.50	98.81	100.0	34.52	100.0	100.0	100.0	69.05	72.62	24.40

F.1.3. INPUT PREPROCESSING

Tabular data are primarily provided in CSV format, with a small number of samples using JSON format. Visual inputs adopt an adaptive preprocessing strategy: for models that support arbitrary resolutions, original images are preserved; when image dimensions exceed model limits, images are resized to the maximum allowable size while maintaining the original aspect ratio; for models that enforce a fixed aspect ratio (e.g., square inputs), non-uniform stretching is applied. Although this operation alters the geometric proportions of the images, it preserves key topological structures and textual forms, thereby ensuring the readability of semantic information.

F.2. Performance of MLLMs on QA

1. Atomic Capability Distribution and Performance Bottleneck Analysis in Multimodal QA Tasks

To systematically characterize the capability structure and performance bottlenecks of models in multimodal QA tasks, we first categorize all questions by task type and further summarize the underlying atomic capabilities they rely on. As shown in Table 4, in both the Metromap and Travelmap scenarios, question difficulty is graded based on the overall performance of different models: questions that almost all models fail to answer correctly are defined as

Hard, questions with significant performance variance across models are categorized as *Medium*, and questions on which most models perform well are labeled as *Easy*. On this basis, we systematically summarize the core atomic capabilities involved in questions of different difficulty levels by jointly considering question semantics and solution procedures.

Experimental results show that the primary performance bottlenecks in multimodal QA tasks are concentrated in **numerical reasoning ability and native intuitive visual reasoning ability**. In contrast, for perceptual tasks such as target localization and retrieval in images and tables, model performance is relatively stable and mature. A clear performance divergence is observed across different types of perceptual and reasoning capabilities.

Specifically, the majority of questions involving counting, numerical comparison, and numerical computation, as well as tasks relying on native intuitive visual reasoning (e.g., path trajectory tracing and trajectory intersection detection), are mainly distributed in the *Hard* and *Medium* difficulty ranges. This result indicates that, in complex QA scenarios, the key bottlenecks of current open-source multimodal models still lie in the insufficient ability to precisely model numerical relationships and the lack of high-level visual intuitive reasoning. In contrast, nearly all questions focused on localization capabilities, whether in image-based tasks that require identifying target elements within images or in table-based tasks that require retrieving corresponding entries from structured tables, and are categorized as *Easy*, reflecting that localization, as a lower-level perceptual skill, has become a widely available and stable strength of existing models.

Further analysis based on Table D2 shows that the most challenging tasks are concentrated in three representative questions: (1) the **M+V-GP** question in the Metromap scenario: “What is the total stop time of the subway line with the longest stop time?”; (2) the **M-GP** question in the Travelmap scenario: “How many tourist attractions are there in total?”; and (3) the **M+V-SR** question in the Travelmap scenario: “What is the cost of the lowest-priced location adjacent to {Spot A}?”

Taken together, the experimental results clearly demonstrate that the core performance bottleneck of current multimodal models in complex QA scenarios lies in their limited **multi-hop reasoning capability**. Although these questions differ substantially in their surface forms, they share a common structural requirement at the capability level: all of them require models to perform cross-modal, multi-step sequential reasoning grounded in complex visual or structured inputs. Unlike tasks that rely on single-step judgments, such problems demand consistent information propagation and integration across multiple intermediate reasoning states. During multi-step reasoning, perceptual errors, relational modeling biases, or numerical instabilities introduced at early stages tend to accumulate and be progressively amplified in subsequent steps, ultimately leading to systemic failure of the entire reasoning chain. Consequently, **the key challenge of multimodal QA does not stem from the deficiency of any individual module, but rather from a structural performance ceiling dominated by error accumulation throughout the multi-hop reasoning process**.

2. Mechanism Analysis of Explicit Chain-of-Thought in Multimodal QA Tasks

Results in Table 5 show that introducing Explicit Chain-of-Thought (CoT) significantly improves overall reasoning performance in multimodal QA tasks, but does not substantially enhance perceptual capabilities.

Specifically, explicit CoT fails to yield noticeable gains in the following task types: (1) **M-GP** in Metromap (Visual perception, Counting); (2) **M-SR** in Metromap (Target localization); (3) **M+V-LP** in Travelmap (Graph trajectory tracing, Target localization, Numerical computation); (4) **M+V-SR** in Travelmap (Target localization, Numerical comparison).

These tasks are primarily limited by insufficient perception and structural understanding at the image or chart level. As perceptual errors accumulate across reasoning steps, explicit CoT cannot effectively translate enhanced intermediate reasoning into final performance gains. This demonstrates that **CoT is only effective when reliable perception has already been established, and cannot compensate for perceptual deficiencies**. Therefore, in complex multimodal QA scenarios, perceptual bottlenecks directly cap the upper bound of performance gains achievable through structured guidance at the reasoning stage.

3. Perception-Domain Ablation Analysis

As shown in Table 6, perception-domain ablation reveals significant differences in how perceptual capabilities affect multimodal QA performance, with **global perception-related tasks constituting the primary bottleneck**. Global Perception-based Reasoning (GP) tasks are heavily concentrated in the *Hard* category (5 Hard, 1 Easy), significantly

exceeding Local Perception-based Reasoning (LP) and Spatial Relationship (SR) tasks, which exhibit either Easy-dominant or balanced distributions. This result indicates that models have already developed relatively stable capabilities for local target localization and local perceptual reasoning; however, once the perceptual scope expands to a global scale, their performance degrades markedly.

From a mechanistic perspective, the high difficulty of global perception tasks primarily stems from their broader perceptual scope and higher structural complexity. Unlike local perception tasks, which require attention to a limited region or a single object, global tasks demand that models integrate multiple dispersed targets and their structural relationships across wide-ranging visual inputs, thereby imposing substantially greater requirements on attention allocation and information fusion. Moreover, global scenes often contain a large amount of irrelevant and distracting information, requiring models to suppress noise while maintaining sustained focus on critical regions. This substantially increases the risk that perceptual errors accumulate during multi-step reasoning, which may ultimately lead to the failure of the entire reasoning process.

In summary, the perceptual-domain ablation analysis reveals the systemic difficulty of global perception tasks and their limiting effect on multimodal QA performance. While models have become relatively mature in local perceptual capabilities, they still exhibit pronounced bottlenecks in large-scale information integration and interference suppression. This finding provides clear guidance for future model improvements, highlighting the importance of enhancing perceptual structural modeling and the robustness of multi-hop reasoning.

Table 5. Difficulty statistics of different questions in the Metromap and Travelmap scenarios. Questions that models almost entirely fail to answer are categorized as “Hard”; questions with substantial performance variance across models are categorized as “Medium”; and questions on which models generally perform well are categorized as “Easy”. Each question is further classified by the underlying capabilities it requires, enabling an analysis of which abilities models still have room to improve.

Metromap-Hard			Metromap-Medium			Metromap-Easy		
Problem	Ability Evaluation		Problem	Ability Evaluation		Problem	Ability Evaluation	
M-LP	Counting		M-GP	Counting		M-SR	Target localization	
E-GP	Numerical comparison, Counting		V-GP	Counting		E-LP	Target localization	
E-SR	Counting		V-LP	Counting		V-SR	Target localization	
M+V-GP	Graph trajectory tracing, Target localization, Numerical computation		M+V-SR	Target localization, Target localization		—	—	
M+V-LP	Graph trajectory tracing, Target localization, Numerical computation		—	—		—	—	
Travelmap-Hard			Travelmap-Medium			Travelmap-Easy		
Problem	Ability Evaluation		Problem	Ability Evaluation		Problem	Ability Evaluation	
M-GP	Visual perception, Counting		M-SR	Target localization, Counting		M-LP	Visual perception	
E-GP	Target localization, Numerical comparison, Counting		E-SR	Target localization, Numerical comparison		E-LP	Target localization	
V-GP	Numerical comparison, Counting		—	—		V-LP	Target localization, Numerical comparison	
M+V-SR	Target localization, Numerical comparison		—	—		V-SR	Target localization, Spatial reasoning	
—	—		—	—		M+V-GP	Counting, Numerical comparison	
—	—		—	—		M+V-LP	Visual planning, Numerical comparison	

Table 6. Statistics of the number of GP, LP, and SR questions under each difficulty level in the Metromap and Travelmap scenarios.

	GP	LP	SR
Hard	5	2	2
Medium	2	1	3
Easy	1	5	3

F.3. Ablation study of Map difficulty and Query difficulty

Figure 4 illustrates in detail the distribution of model accuracy across different input modalities as a function of Map Difficulty and Query Difficulty. We observed distinctly different performance decay patterns between the two datasets:

- Polarized Performance and Reasoning Collapse in Metromap:** In the Metromap scenario, the accuracy distribution exhibits significant **imbalance**. Models perform reasonably well on “Easy” samples, but experience a **precipitous drop** on “Medium” and “Hard” levels, with accuracy for “Hard” samples approaching zero. This phenomenon indicates that the high-level topological structures in Metromap, such as complex transfer networks and densely connected nodes, have reached or even exceeded the **cognitive capacity ceiling** of current models. Once the graph complexity surpasses a critical threshold, the reasoning ability collapses systematically rather than declining gradually.
- Linear Decay and Adaptivity in Travelmap:** In contrast, Travelmap shows a more stable performance across difficulty levels, exhibiting a uniform distribution. Although accuracy decreases with increasing difficulty, the decay curve remains gradual without functional failure. This suggests that the topological logic in Travelmap, even in the Hard mode, largely remains within the models’ effective reasoning boundary, allowing them to maintain relatively stable generalization capabilities.

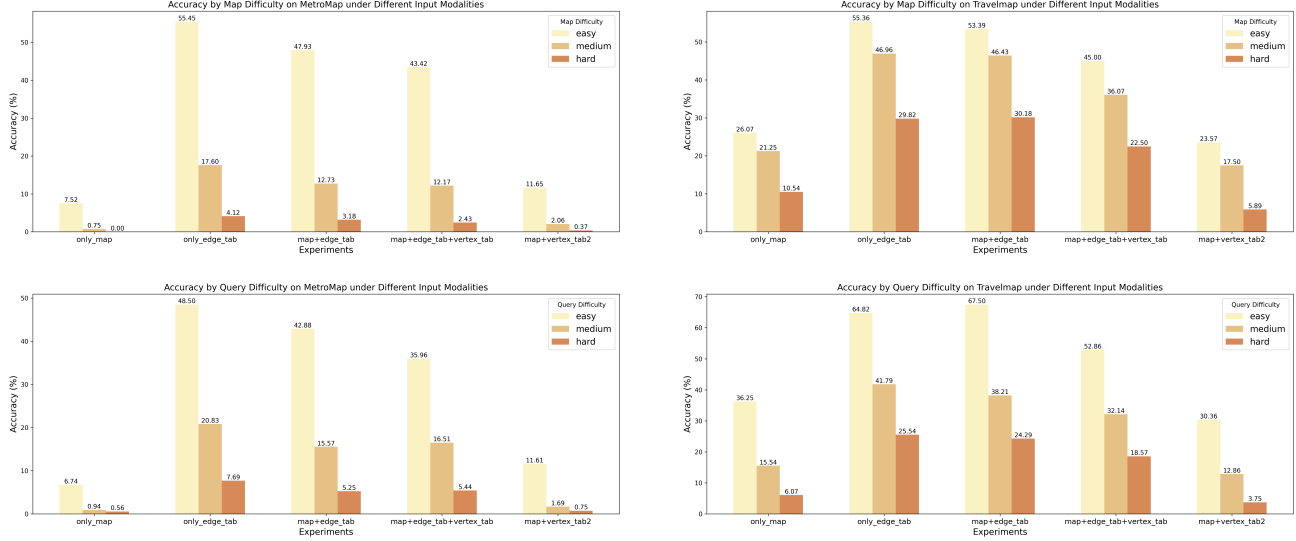


Figure 4. Distribution of model accuracy across Map Difficulty and Query Difficulty under different input modalities (Metromap and Travelmap scenarios).

Through a cross-analysis of Map Difficulty and Query Difficulty, Figure 5 presents a more fine-grained distribution of performance gradients. Overall, model accuracy exhibits a pronounced stepwise decline as task complexity increases, progressively degrading from the Easy-Easy combination to the Hard-Hard combination.

Further fine-grained analysis reveals clear differences in sensitivity to the sources of complexity across task scenarios. In the Metromap task, map topological complexity has a significantly greater impact on final performance than query logical complexity, indicating that the overall visual complexity and information density of metro network diagrams constitute the

MapTab: Can MLLMs Master Constrained Route Planning?

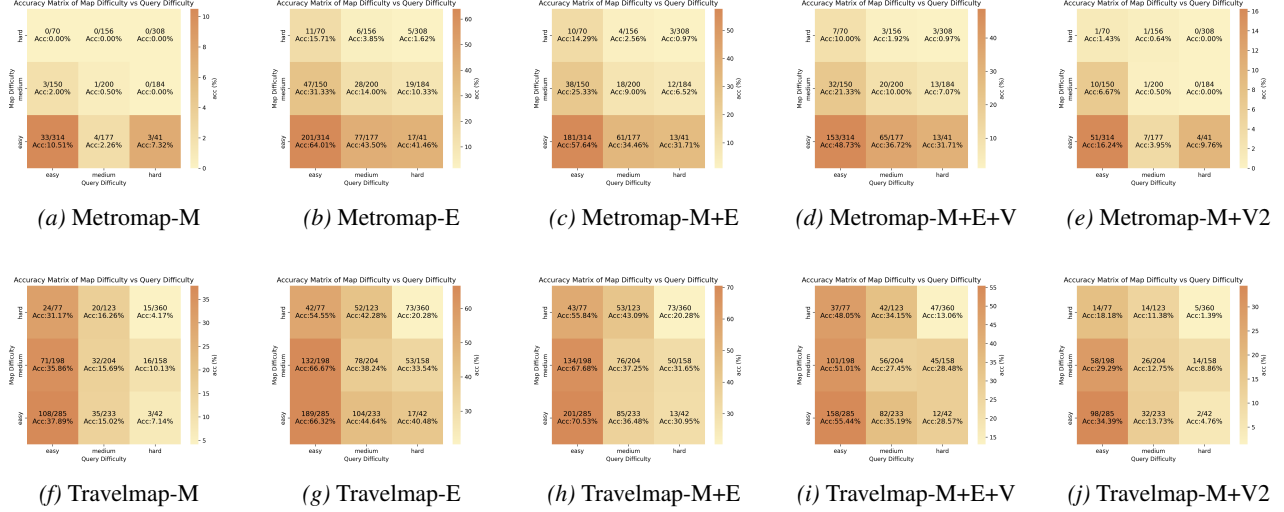


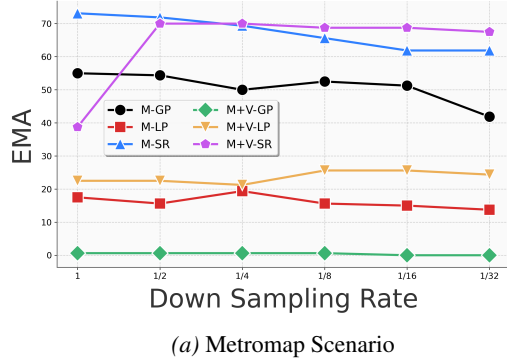
Figure 5. Model accuracy matrix under different combinations of Map Difficulty and Query Difficulty. The first row shows results in the Metromap scenario, while the second row corresponds to the Travelmap scenario. M denotes Map Only; E denotes Edge Table Only; M+E denotes Map + Edge Table; M+E+V denotes Map + Edge Table + Vertex Table; and M+V2 denotes Map + Vertex₂_tab.

primary challenge. In contrast, in the Travelmap task, query logical complexity exerts a substantially stronger influence on performance than map topological complexity, suggesting that the reasoning structure of the queries and multi-step logical composition are the key limiting factors in this scenario.

These results demonstrate that the dominant factors constraining model performance vary across task scenarios. Consequently, distinct optimization strategies are required for scenarios dominated by perceptual complexity versus those dominated by reasoning complexity.

F.4. Ablation study of QA for resolution

Impact of Image Resolution on QA in Metromap



Impact of Image Resolution on QA in Travelmap

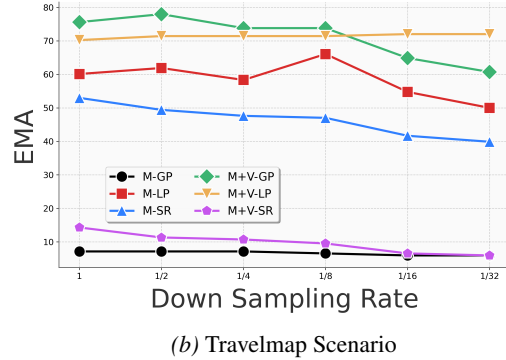


Figure 6. Effects of different image resolutions on QA task performance in the Metromap (a) and Travelmap (b) scenarios. Images are proportionally downsampled to 1/2, 1/4, 1/8, 1/16, and 1/32 of the original resolution. Evaluation is conducted under six Map-based input settings: Map-GP (M-GP), Map-LP (M-LP), Map-SR (M-SR), Map+Vertex_{tab}-GP (M+V-GP), Map+Vertex_{tab}-LP (M+V-LP), and Map+Vertex_{tab}-SR (M+V-SR).

For QA queries, experimental results indicate that improvements in image clarity are not a sufficient condition for enhancing model performance. On the contrary, for multiple categories of questions, moderately downsampled images often lead to better reasoning outcomes. In some tasks, model accuracy even exhibits a stable upward trend as the degree of downsampling increases. This phenomenon suggests that the sampling rate itself is not the key determinant of model performance. Instead, model behavior is more strongly constrained by the perceptual granularity and reasoning paradigm required by the specific task. When a task primarily relies on global structural understanding or high-level semantic abstraction, reducing

visual redundancy can help suppress irrelevant details, thereby enabling the model to focus more effectively on information that is critical for reasoning.

F.5. Ablation study of Tabular Modality

Experimental Setup. We adopt two table formats, namely CSV and JSON, for the tabular modality. Table 7 reports the token counts of three table types, including Edge_tab, Vertex_tab, and Vertex2_tab, under both formats. In addition, Table 7 investigates the performance of CSV and JSON formats in two constraint-aware RP settings, namely Map+Edge_tab+Vertex_tab and Map+Vertex2_tab, analyzing whether different table representations affect the model’s perception and understanding of tabular content. Table 8 further presents comparative experimental results of the two formats on QA queries.

Experimental Results. We initially hypothesized that the JSON format would provide stronger structural cues and thus improve model understanding and overall performance, whereas the CSV format, despite being more token-efficient, might suffer from weaker interpretability. However, experimental results reveal that although the CSV format uses more than 50% fewer tokens than the JSON format, its performance is not inferior in either RP or QA tasks, and even outperforms JSON in certain cases. This indicates that while the JSON format offers richer structural information, it does not increase the upper bound of model perception and reasoning capabilities. On the contrary, the longer context induced by JSON representations may sometimes hinder reasoning performance.

Table 7. Token counts under CSV and JSON table formats and their performance comparison on RP queries.

Input format	Token Statistics			Map+E_tab+V_tab			Map+V2_tab		
	E_tab	V_tab	V2_tab	EMA	PMA	DS	EMA	PMA	DS
Metromap									
csv	2651	2264	2496	19.75	40.16	876	6.31	24.48	255
json	6465	6193	6397	19.31	39.31	855	4.69	21.87	182
Travelmap									
csv	577	462	462	33.39	55.10	1929	15.42	40.83	800
json	1299	1131	1131	34.52	55.56	2002	15.65	40.97	804

Table 8. Performance comparison of CSV and JSON table formats on QA queries.

Input format	E-GP	E-LP	E-SR	V-GP	V-LP	V-SR	M+V-GP	M+V-LP	M+V-SR
	(Acc)								
Metromap									
csv	20.00	100	3.12	47.50	58.75	78.75	1.25	21.25	70.00
json	22.50	100	7.50	57.50	51.88	86.88	0.63	22.50	38.75
Travelmap									
csv	19.64	99.40	44.05	25.00	47.02	54.17	76.19	72.02	16.07
json	17.86	99.40	45.24	38.69	50.60	61.31	75.60	70.24	14.29

F.6. Ablation study of Language

Figure 7 presents the overall language distribution in the Metromap and Travelmap scenarios using a mixed statistical approach, retaining only the top five categories by proportion and aggregating the remaining categories. Figure 7a shows the distribution of the native language of the locations corresponding to the images, covering a total of 328 images. The results indicate that locations with Chinese as the native language account for the highest proportion at 52.1%, followed by English at 24.4%. Figure 7b further summarizes the actual language used in the images, also based on 328 images, showing a distribution trend similar to that of the native language statistics, with Chinese being the most frequently used and English second. Based on these observations, Figure 7c categorizes the languages into Chinese, English, and Others,

MapTab: Can MLLMs Master Constrained Route Planning?

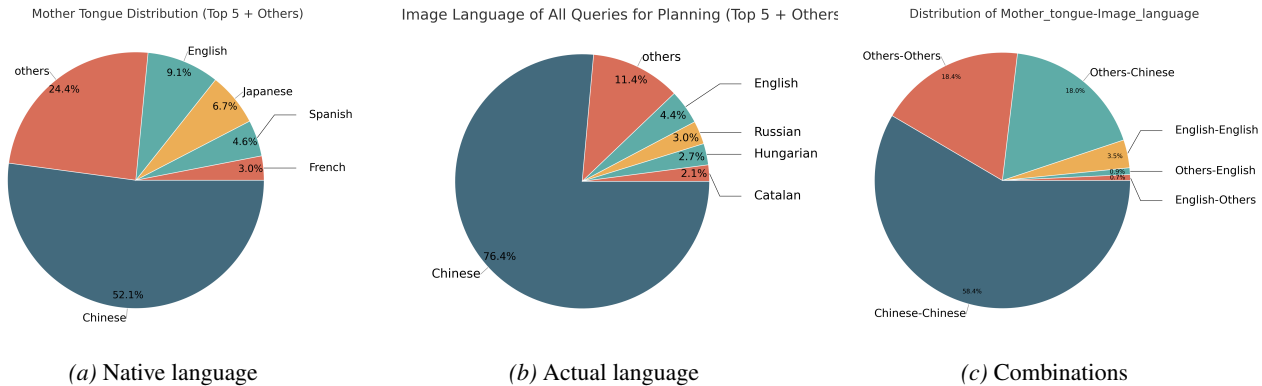


Figure 7. All images have the exact same height. Widths are adjusted automatically.

denoted as Chinese, English, and Others, respectively, and further divides them into nine combinations according to the mother_tongue-image_language pairing. Since the combinations Chinese-English, Chinese-Others, and English-Chinese do not appear in the data, the analysis focuses on the remaining six categories. The results show that the Chinese-Chinese combination has the highest proportion at 58.4%.

Experimental results in Table 9 indicate a significant language bias in model performance: across regional datasets, when the input uses a dominant language (Chinese or English), the model consistently performs better than in cases using other languages. This phenomenon is highly correlated with the frequency distribution of different languages in the training corpus, reflecting the model’s stronger adaptation to high-frequency languages. Meanwhile, the model does not exhibit a significant language prior based on geographic or regional knowledge. When the native language of the location corresponding to the image does not match the language actually used in the data, model performance does not show systematic variation, indicating that the key factor affecting model performance is the language used in the sample itself rather than the native language attribute of the location.

Table 9. Experimental performance results under different language distributions in the Metromap and Travelmap scenarios.

Model and Constraint Settings	Chinese-Chinese		English-English		Others-Others		Others-Chinese		Others-English		English-Others	
	EMA	PMA	EMA	PMA	EMA	PMA	EMA	PMA	EMA	PMA	EMA	PMA
Qwen3-map	12.10	31.65	6.03	22.85	2.64	19.47	18.31	38.81	17.86	43.18	0	13.17
Qwen3-map+e_tab	30.78	47.77	31.03	56.41	29.92	53.61	41.36	60.79	57.14	71.25	4.17	33.70
Qwen3-map+e_tab+v_tab	26.29	44.86	32.76	52.13	23.80	48.53	31.36	54.22	60.71	76.29	4.17	29.93
Qwen3-map+v2_tab	10.59	31.30	7.76	27.07	5.12	26.07	15.25	39.19	17.86	48.41	0	18.23
GPT4o-map	11.42	31.23	15.52	34.51	8.26	33.63	15.42	39.05	28.57	59.34	12.50	37.30
GPT4o-map+e_tab	49.71	63.21	55.17	75.92	46.61	73.51	61.86	76.77	96.43	98.66	58.33	76.84
GPT4o-map+e_tab+v_tab	37.14	53.46	61.21	74.75	42.15	66.64	47.46	66.93	57.14	75.49	41.67	70.84
GPT4o-map+v2_tab	9.49	30.23	25.00	46.14	14.05	40.25	13.56	40.51	14.29	47.60	46.67	35.21

G. Error Case Analysis

Based on the experimental results, after excluding anomalies caused by repeated generation or answer collapse in certain small-scale open-source models (Yao et al., 2025), we randomly sampled and analyzed 100 erroneous predictions from the entire set of errors, with 50 from models with explicit reasoning mechanisms and 50 from models without. Systematic analysis indicates that these errors mainly reflect three key deficiencies in current vision-language models: shortcomings in instruction-following ability, insufficient symbolic visual perception, and imbalanced reasoning capabilities.

First, some small-scale open-source vision-language models exhibit significant issues in following instructions in complex scenarios. Our chart-modality collaborative multi-constraint RP tasks involve high input complexity, consisting of a map image, two structured tables, and multiple fine-grained, interrelated constraints (as described in E.2), including explicit definitions of start and end points, fixed output formats, and multi-factor weighting. For small-scale open-source models (e.g., Qwen3-VL-8B), the overall ability to follow multiple complex instructions under long-context conditions remains limited, especially when it comes to consistently adhering to key constraints that are concise yet critical for correctness.

Specifically, Qwen3-VL-8B in some samples even misinterpreted the basic definitions of start and end points (see Figure 8); in other samples, although the model successfully inferred the correct path, it failed to comply with the instruction to annotate “(transfer)” after transfer stations, leading to outputs being judged as incorrect (see Figure 9).

Second, even highly capable vision models continue to encounter challenges in fine-grained symbolic reasoning. Unlike object-centric natural images, the subway and tourist maps we use are essentially highly structured graphical visual representations, with core information encoded as topological relationships and symbolic logic. Natural images typically exhibit “sparse information, dense features,” e.g., a rectangular region containing a cat has many contiguous pixel features supporting the recognition of object class, appearance, and texture. In contrast, subway and tourist maps often have large blank backgrounds and sparse low-level visual features, yet extremely high information density: a single area may contain multiple overlapping lines of different colors, with intersections overlaid with transfer station names and adjacent line labels. Therefore, these tasks require the model to possess near-human symbolic visual perception, i.e., to accurately parse and track visual information in complex stacking and irregular layouts with symbols as the focus. However, error analysis shows that this ability remains generally insufficient in current models. Even high-performance closed-source models such as Gemini-3-Flash sometimes fail to consistently and accurately track continuous subway line trajectories (see Figure 10); in areas with dense multiple lines, the model may exhibit “line-jumping,” i.e., jumping unrealistically from one line’s station to another’s (see Figure 11).

Finally, vision-language models exhibit a dual imbalance in reasoning: “overthinking simple problems and underthinking complex problems.” After excluding perception factors, error analysis further revealed two typical reasoning issues. On the one hand, some models with explicit reasoning mechanisms tend to overthink relatively simple tasks, leading to performance degradation. As shown in Figure 12, for a problem with Map_Difficulty = Easy, Query_Difficulty = Medium, and Difficulty_score = 3, Qwen3-VL-Plus can directly produce the correct answer without the reasoning mechanism enabled; however, enabling the reasoning mechanism results in errors. Detailed analysis of its reasoning process shows that the model performed up to 25 `wait` operations, frequently doubting, self-correcting, and switching thought paths, which not only reduced reasoning efficiency but also truncated the reasoning process and interfered with an originally correct solution. On the other hand, for reasoning problems requiring explicit comparison of multiple attributes and constraint optimization, the current models’ computation and reasoning capabilities are still insufficient. As shown in Figure 13, even with only two candidate paths, Gemini-3-Flash failed to accurately calculate and compare the relevant attribute values to select the optimal path satisfying the constraints, instead resorting to approximate guessing based on the shortest path.

H. Limitations

Despite providing a high-quality multimodal benchmark, this study has several limitations:

1. *Limited Map Diversity.* The current evaluation is limited to topological graph scenarios, such as metro and attraction maps. In principle, more complex cartographic representations, including large-scale urban maps or remote sensing maps, could also be transformed into heterogeneous graphs for systematic assessment. Extending MapTab to these richer map types would enhance the generality and applicability of the framework.
2. *Lack of Dynamic Evaluation.* This study primarily relies on static maps and predefined constraints, without incorporating dynamic environments or real-time information updates. Future research should examine model performance under temporally evolving conditions, where constraints and graph structures may change in real time, to better simulate realistic decision-making scenarios.
3. *Deficiencies in Model Reasoning.* Experimental results indicate that current MLLMs still exhibit notable deficiencies in complex visual perception, multi-dimensional constraint parsing, and long-tracing numerical or compositional reasoning. These findings highlight the need for future model development to prioritize improvements in these core capabilities, thereby enhancing robustness, generalization, and overall reasoning performance in multimodal, multi-constraint tasks.

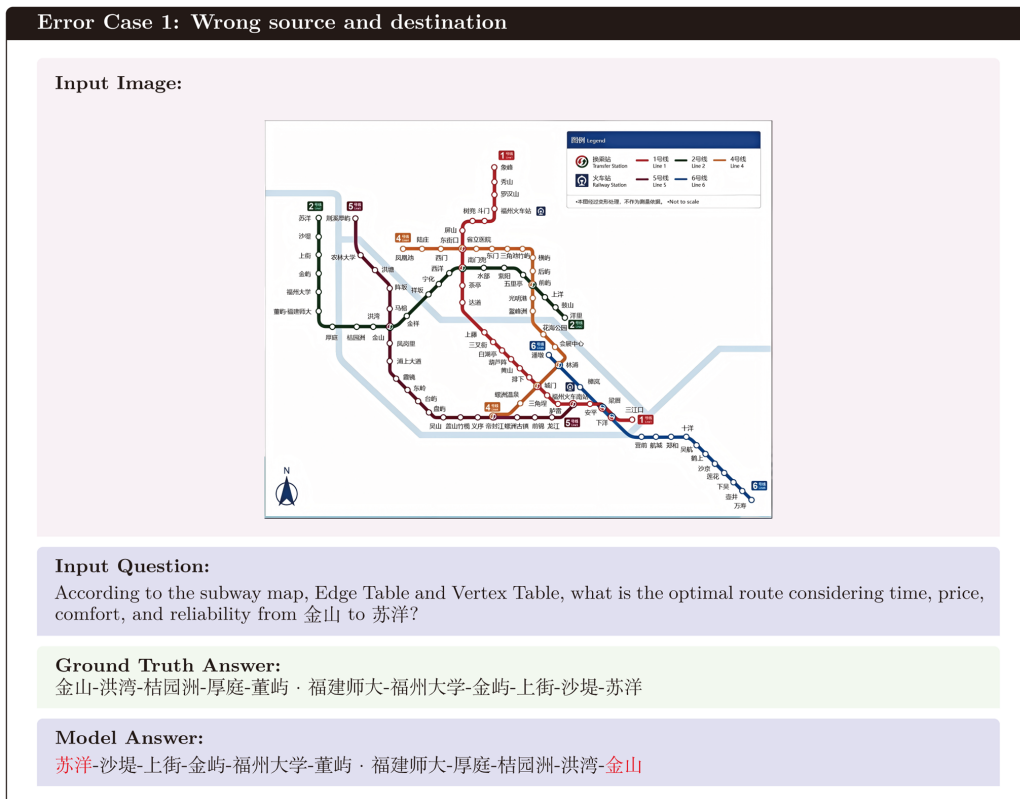


Figure 8. Error Case 1: Wrong source and destination



Figure 9. Error Case 2: Missed Transfer Label

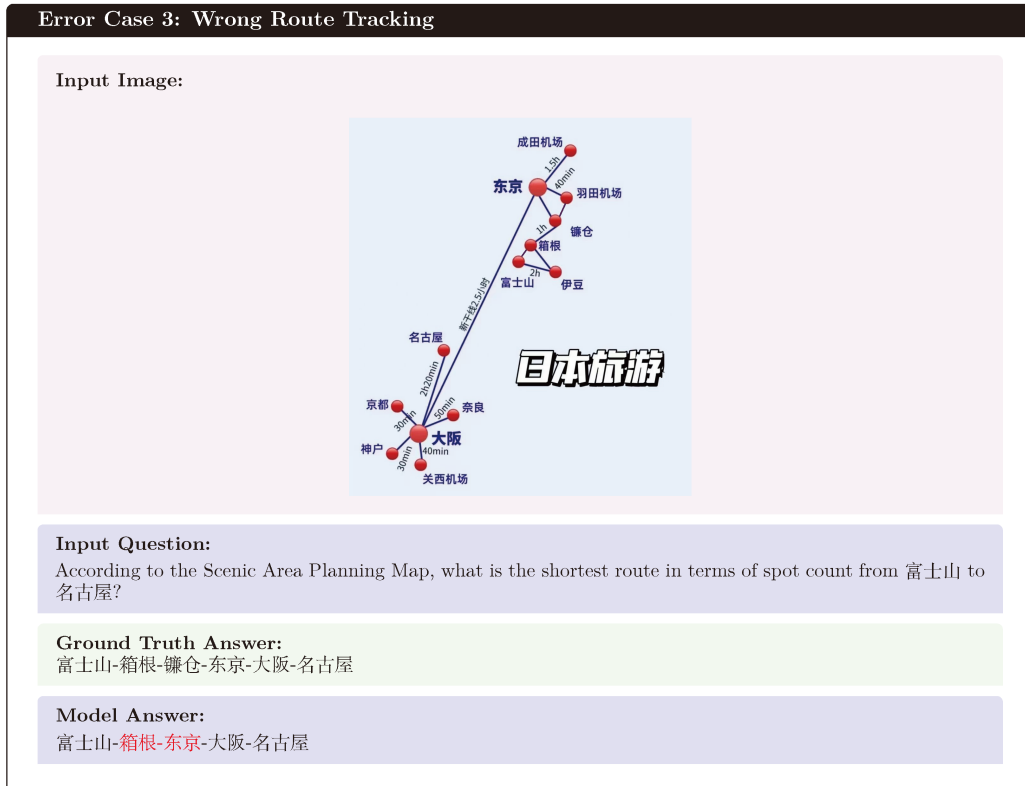


Figure 10. Error Case 3: Wrong source and destination

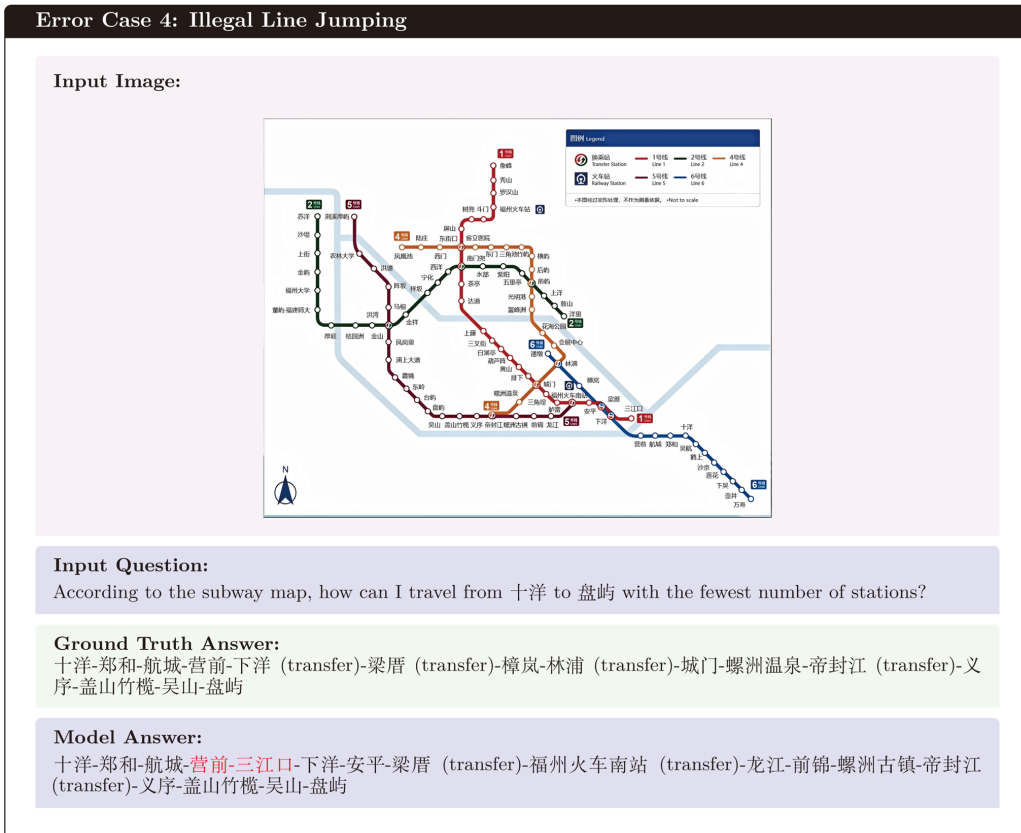


Figure 11. Error Case 4: Illegal Line Jumping

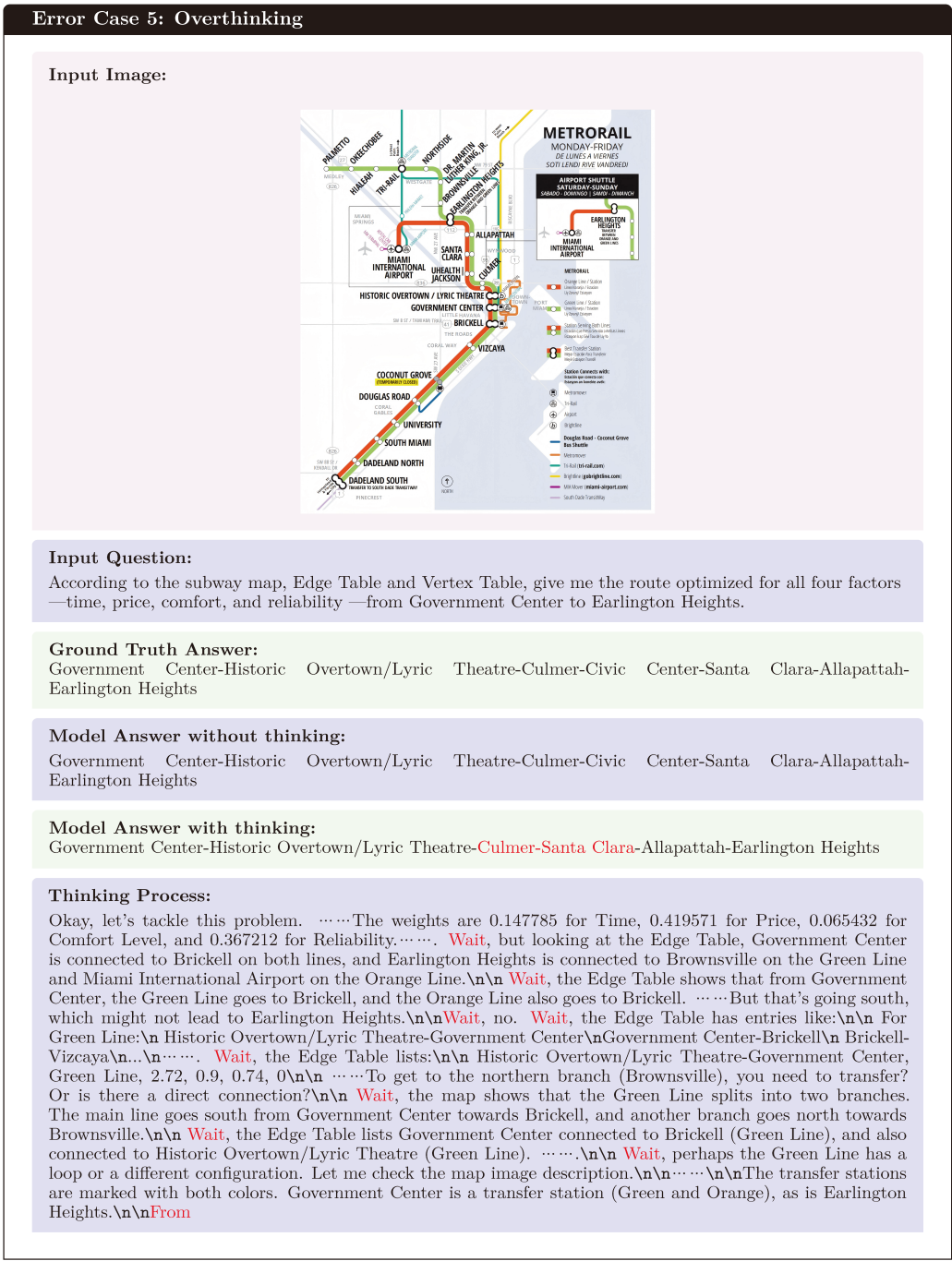


Figure 12. Error Case 5: Overthinking



Figure 13. Error Case 6: Failed Constrained Reasoning